THESIS FOR THE DEGREE OF DOCTOR OF PHILOSOPHY

Short- and long-term variability in future electricity systems

– Ensuring the flexibility to manage the grid frequency and inter-annual variations

JONATHAN ULLMARK

Department of Space, Earth and Environment

CHALMERS UNIVERSITY OF TECHNOLOGY

Gothenburg, Sweden 2024

Short- and long-term variability in future electricity systems
– Ensuring the flexibility to manage the grid frequency and inter-annual variations

JONATHAN ULLMARK
ISBN 978-91-8103-005-1

Doktorsavhandlingar vid Chalmers tekniska högskola
Ny serie nr 5463
ISSN 0346-718X

Department of Space, Earth and Environment
Chalmers University of Technology
SE-412 96 Gothenburg
Sweden
Telephone + 46 (0)31-772 1000

Printed by Chalmers Reproservice
Gothenburg, Sweden 2024

Short- and long-term variability in future electricity systems

– Ensuring the flexibility to manage the grid frequency and inter-annual variations

JONATHAN ULLMARK
Division of Energy Technology
Department of Space, Earth and Environment
Chalmers University of Technology

ABSTRACT

To achieve climate mitigation targets, the net climate impact from electricity generation must be drastically reduced in the near future, and eventually eliminated. The level of generation must also be increased to accommodate the increasing demand as the transport and industry sectors undergo electrification. However, the ongoing transition to weather-dependent electricity generation poses challenges in terms of providing ancillary services and ensuring security-of-supply in the electricity system.

This thesis applies techno-economic optimisation modelling to investigate two challenges related to non-dispatchable generation from wind power and solar photovoltaics (PV): (i) the cost-effective provision of sufficient short-term flexibility to control the grid frequency; and (ii) the cost-effective provision of long-term flexibility to manage inter-annual variability. This investigation is focused on identifying the key technologies that may provide the two forms of flexibility and on whether the cost-optimal mix of technologies to supply electricity is affected. This is achieved using a linear electricity system model that optimises the installed capacity levels and the operation of generation and storage technologies. Specifically, the model encompasses nuclear and bio-fuelled thermal power, wind power and solar PV, Li-ion batteries, hydrogen storage systems, and heat-generation technologies for inter-connected district heating systems. Electricity transmission between neighbouring regions is also modelled in **Papers II–IV**.

It is found that batteries play a key role in limiting the cost of providing flexibility for grid frequency control, although other technologies, such as hydro- and thermal power, curtailed wind and solar power and flexible power-to-heat for district heating, also contribute. The results indicate that, with grid-scale batteries as an investment option, the demand for inertia and reserve power availability would increase the system cost by 0.5 €/MWh of produced electricity. However, the results also show decreasing costs as the shares of wind power and solar PV increase, and that a weaker impact on system cost can be achieved if reserve power is provided by flexible household loads.

In terms of inter-annual variability, the results support previous studies that have demonstrated that the levels of cost-optimal investments generated by individually modelled weather-years vary widely (e.g., total thermal capacity is in the range of 74–141 GW in Northern Europe). Furthermore, the results show that accounting for inter-annual variability affects only slightly the total capacity levels of wind, solar and nuclear power. However, inter-annual variability increases the capacities of biogas turbines and may increase the need for long-term biogas storage.

Keywords: Electricity systems modelling, capacity expansion planning, battery storage, flexibility, inter-annual variability, frequency control

LIST OF PUBLICATIONS

The thesis is based on the following appended papers, which are referred to in the text by their assigned Roman numerals:

I. J. Ullmark, L. Göransson, P. Chen, M. Bongiorno, and F. Johnsson, "Inclusion of frequency control constraints in energy system investment modeling," *Renew. Energy*, vol. 173, pp. 249–262, Aug. 2021, doi: 10.1016/j.renene.2021.03.114.

II. J. Ullmark, L. Göransson, and F. Johnsson, "Frequency reserves and inertia in the transition to future electricity systems," *Energy Syst.*, Feb. 2023, doi: 10.1007/s12667-023-00568-1.

III. J. Ullmark, L. Göransson, and F. Johnsson, "Potential revenue from reserve market participation in wind power- and solar power-dominated electricity grids," accepted for publication in *Int. J. Energy Res*.

IV. J. Ullmark, L. Göransson, and F. Johnsson, "Representing Net Load Variability in Electricity System Capacity Expansion Models - Accounting for Challenging Net-Load Events," submitted for publication, doi: 10.2139/SSRN.4681508

Jonathan Ullmark is the principal author of all the papers. Professor Filip Johnsson and Associate Professor Lisa Göransson contributed with discussions and editing of all the papers. Professor Massimo Bongiorno and Associate Professor Peiyuan Chen contributed with discussions and editing of **Paper I**.

Other publications by the author, not included in the thesis:

P. Holmér, J. Ullmark, L. Göransson, V. Walter, and F. Johnsson, “Impacts of thermal energy storage on the management of variable demand and production in electricity and district heating systems: a Swedish case study,” *Int. J. Sustain. Energy*, vol. 39, no. 5, pp. 446–464, May 2020, doi: 10.1080/14786451.2020.1716757.

M. Lehtveer *et al.*, “Actuating the European Energy System Transition: Indicators for Translating Energy Systems Modelling Results into Policy-Making,” *Front. Energy Res.*, vol. 9, p. 677208, Sep. 2021, doi: 10.3389/fenrg.2021.677208.

ACKNOWLEDGEMENTS

Sometimes, when I hear about the experiences and struggles of PhD students in other research groups, I realize how fortunate I was. It seems to be the rule, rather than the exception, that aspiring PhD students know too little to properly evaluate their prospective workload, workplace, supervisor, and research groups. I was fortunate to have interacted with Lisa Göransson, Viktor Walter, Mikael Odenberger, Maria Taljegård, Dmytro Romanchenko, and Mariliis Lehtveer in my studies before seeking a PhD position in their research group. I was also lucky that the impression these individuals gave me beforehand was not too far off the mark. As such, the challenges and struggles I encountered were manageable, and they helped me develop in an environment that was safe, friendly, and supportive. It breaks my heart that it is not just a rare story heard at some conference in second-hand, about PhD students who end up in unsafe or unsupportive environments.

That being said, I am especially grateful to my main supervisors, Lisa Göransson and Filip Johnsson. Thank you, Lisa, for the numerous deadlines, for helping me build an intuition for models and model results, and for showing me how to design a course with effective and inclusive teaching. Thank you, Filip, for your wisdom and for never letting your vast workload get in the way of offering an open invitation for support and discussions. I am also thankful to Peiyuan Chen and Massimo Bongiorno for sharing their electric power engineering perspective, knowledge and intuition in the early phases of this project, when I needed it the most. Viktor Walter, my first modelling supervisor, thank you for all of our talks – especially the non-modelling ones.

To my colleagues at the Division of Energy Technology, thank you for the friendly atmosphere and the many fikas. It became especially clear during the pandemic that there is a world of difference between working alone and working individually. To the energy system modelling group, thank you for making the work individual instead of lonely, and for the many interesting discussions. Special thanks to Alla Toktarova, Hyunkyo Yu and Maria de Oliveira Laurin for making the office not just friendly, but fun.

Marie Iwanow, thank you for your patience, kindness and consistent efforts to assist and accommodate us at the division. I appreciate that there always was something for me at fikas and events, even when I was the only vegan in the division.

Finally, I am thankful for the support and love from my family. Though I have periodically found myself single-mindedly focusing on work, it has been a great comfort to know that you are always there for me when I need you.

Göteborg, 6th of February 2024

ABBREVIATIONS

AC	Alternating current
BECCS	Bio-energy with carbon capture and storage
CCGT	Combined cycle gas turbine (also referred to as ‘mid-load’)
CCS	Carbon capture and storage
CDR	Carbon dioxide removal
CTPC	Chronological time-period clustering
DACCS	Direct air carbon capture and storage
DC	Direct current
ESM	Electricity system model
FC	Frequency control
FCR	Frequency containment reserves
FFR	Fast frequency reserves
FR	Frequency reserves
FRR	Frequency restoration reserves
aFRR	Automatic FRR
mFRR	Manual FRR
GEP	Generation expansion model
MIQCP	Mixed integer quadratically constrained program
OCGT	Open cycle gas turbine (also referred to as ‘peak-load’)
PCTPC	Priority chronological time-period clustering
RD	Representative day
RE	Renewable energy
RPM	Rotations per minute
RR	Replacement reserves
RTS	Representative time-series
RoCoF	Rate of change of frequency
TSA	Time-series aggregation
VRE	Variable renewable electricity

TABLE OF CONTENTS

1. INTRODUCTION

Decarbonisation of the world's energy systems has become a major focus of the global community. To this end, 195 signatories agreed in 2015 to the Paris Agreement, defining a shared goal and responsibility to limit global warming to well below 2°C above pre-industrial levels, with efforts to be made to limit the global temperature increase to 1.5°C. During the writing of this thesis, 8 years after the Paris Agreement, the global temperature increase exceeded 2°C for the first time ever, for two days in November of 2023 [1]. Two days of abnormally high temperatures do not mean that the Paris Agreement has already failed, although it set a sobering atmosphere for the 2023 United Nations Climate Change Conference (COP28), which was held just 2 weeks later in Dubai. One result of COP28 was a call upon parties to contribute to transitioning away from fossil fuels in energy systems, so as to achieve net-zero greenhouse gas (GHG) emissions by Year 2050 [2]. Although vaguely formulated and only targeting energy systems, this is the first time that the phasing out of fossil fuels is explicitly called for by a UN climate summit [3]. Carbon-neutral electricity is, however, not only needed to replace fossil fuel-fired electricity. Electrification is crucial to limit the GHG emissions from other sectors, such as transportation and steelmaking. Another result of COP28 is a call for contributions to triple the capacity of global renewable energy (RE) by Year 2030.

Of the 348 GW of renewable power capacity added globally in Year 2022, wind power and solar PV constitute 92% [4]. Transitioning to electricity generation that is dominated by wind power and solar PV raises novel technical challenges owing to some key differences compared to traditional thermal power plants. Although there is more than one way to categorise these differences and the resulting challenges, they relate to the following three properties of wind power and solar PV: weather-dependence (i.e., non-dispatchability); grid interface through inverters (thus, no inherent contribution to grid stability); and different conditions for geo-spatial placement. The research presented in this thesis concerns two technical challenges that arise mainly from the non-dispatchability of wind power and solar PV: 1) maintaining at all times sufficient reserve power for grid frequency control; and 2) managing the inter-annual variability of the load and weather-dependent generation.

The weather-dependent, non-dispatchable nature of wind power and solar PV affects the electricity system in different ways as their shares of the yearly supply increase. Since the electricity grid must always maintain a balance between generation and load, flexibility on multiple timescales is vital to ensure the reliability and stability of the electricity grid. This flexibility must allow real-time load balancing to control the grid frequency, while also being capable of dealing with hourly to yearly variations in load and weather-dependent generation. Furthermore, as fossil-based thermal power is replaced by variable generation from wind power and solar PV, flexibility from dispatchable generation is reduced, while the need for flexibility increases. However, in addition to thermal and reservoir hydropower plants, flexibility can be provided by grid-scale batteries, hydrogen storage units, strategic charging of electric vehicles,

and coupling with other sectors. As these flexibility measures exhibit different properties in terms of power, duration, and cost, they take on different roles in managing the electricity net-load (load minus non-dispatchable generation). The need for flexibility measures to support the integration of non-dispatchable generation represents an additional cost to the system, as well as a challenge in terms of ensuring that sufficient flexibility is available for each type of variability.

In the scientific community, decarbonisation and integration of wind and solar power are topics that have attracted increasing interest, especially in the last couple of years [5]. As the integration of wind and solar power has progressed, both current and projected investment costs have fallen, and more research has focused on the design and operation of electricity systems that contain high shares of wind and solar power. Much of this research has included hourly variability on time-scales of up to 1 year. However, due to model limitations, intra-hourly and inter-annual variability have been studied less-intensely. Breyer et al. [6], in a review of the research on 100% RE systems in Year 2022, have pointed out that the last few years have seen some papers published that are critical of the research conducted on 100% RE systems. Perhaps most notably, Heard et al. [7] have argued in a contentious review (published in 2017) that previous research has not sufficiently proven that 100% RE systems are feasible. The review of Breyer et al. summarises and addresses the challenges raised by Heard et al. [7] and others, leading to the identification and discussion of 13 knowledge gaps within the field of 100% RE systems. Two vital aspects that were raised by Heard et al. and included in the list of research gaps by Breyer et al. are inter-annual variability and grid stability, both of which relate to solar PV and (most) wind power being non-dispatchable and inverter-based (i.e., non-synchronous). In this work, only the frequency control aspect of grid stability is considered as it is the only ancillary service requiring active power, thereby directly interacting with the supply of electricity. In addition, reactive power for voltage control can be provided by inverters or so-called 'synchronous condensers' [8]–[10].

1.1 Aim and scope

The aim of the research presented in this thesis is to investigate the extent to which the flexibility that is required in relation to frequency control and inter-annual variability affects the cost, design and operation of future carbon-neutral electricity systems. This is addressed using linear optimisation modelling, with a particular focus on identifying the key technologies. The contributions of **Papers I–IV** are summarised in the following sub-section.

To define the electricity demand, heating demand, industry electrification, renewable resources and existing infrastructure, the modelling in this work uses data for various regions in Europe. The geographical, temporal and technological scopes are described in detail in Section 3.1 (see, in particular, Table 1). To ensure that the model size is tractable, frequency control and inter-annual variability are investigated separately. While a representation of the existing generation capacity is used in **Papers II–IV**, planned projects have not been considered except in the case of transmission capacity.

1.2 Contribution of this work

In **Paper I**, a methodology is developed to represent linearly the demand and supply of grid inertia and frequency reserves in an electricity generation capacity expansion model. The

model is then applied to four isolated and geographically distinct regions for Year 2050, to investigate the impacts of inertia and reserve demands on the cost-optimal system design and operation. It is found that the reserve demand has a greater impact than the demand for grid inertia, and that increased battery investments is the main effect on the system.

In **Papers II** and **III**, the methodology developed in **Paper I** is combined with model development to enable inter-regional electricity trade and a modelled transition of the electricity generation system. The transition is approximated by modelling multiple years in succession, forwarding investments from one year to the next, while taking into account the lifetimes of already existing real-world and modelled investments. By investigating the transitioning systems with and without demands for inertia and frequency reserves, it is found in **Papers II** and **III** that the main effect on the electricity supply is a *slight* increase in the share of electricity from wind and solar power when taking into account frequency control. In the early stages of the transition, the demand for frequency reserves can drive battery storage investments, which in turn decreases the need to curtail variable renewable electricity (VRE).

Paper IV presents and evaluates an algorithm designed to identify representative sets of weather-years, and also analyses how particularly challenging weather-events affect the cost-optimal capacity mix. The latter analysis compares the cost-optimal capacity mix when modelling single, challenging weather-years or multiple weather-years wherein the challenging years have weights that represent their probabilities of occurrence. It is found that these challenging weather events, when their probabilities of occurrence are represented, affect the usage of peak thermal power and the dimensioning of biogas storage units, but not the levels of investment in wind, solar or nuclear power.

1.3 Limitations

The methodology in **Papers I–IV** is limited mainly by factors related to the use of optimisation modelling. Although many compromises are needed (and limiting) in research based on techno-economic energy systems modelling, the ones with highest relevance for this work can be grouped as follows:

- Perfect foresight
- Model size and complexity
- Access to input data

As for all model-based research, the limitations of the models require that the research questions be narrowed to what the model can accurately represent. For **Papers I–IV**, the research is, thus, mainly focused on changes in cost-optimal investment levels and the roles of different technologies in providing grid frequency support or inter-annual flexibility. Additional scenarios are constructed and evaluated to gauge the extents to which the key results are affected by the limitations. A detailed discussion of the limitations and how they affect the research can be found in each of **Papers I–IV**, and an overview is provided in Section 5.2 of this thesis.

2. BACKGROUND AND RELATED WORK

Variability in the electricity system pertains to real-time grid frequency control, the inter-day and intra-day planning of electricity generation, and the long-term planning of hydropower and fuel storage facilities. The sources of variability vary similarly, from sudden unexpected loss of generation (or load) to the stochastic load variations from electricity consumers to the variability inherent to generation from weather-dependent sources, such as wind, solar and run-of-river power plants.

Depending on the duration, amplitude and recurrence of a specific variation in the electricity system, the choice of suitable flexibility technology or strategy may change. For example, the daily high-amplitude, low-duration generation from solar PV requires a flexibility measure that entails a relatively low cost for power (such as battery storage systems or flexible residential heating/cooling), whereas a short storage duration or a high cost for energy storage capacity is acceptable. This type of functionality-based (as opposed to technology-based) categorisation has been used in previous studies that have examined specifically the interactions between flexibility measures and cost-effective pairings of variability sources and flexibility measures [11]–[15]. Electricity system modelling, which is a popular and useful tool for studying the cost-efficient design and operation of electricity systems, is described in Section 2.1.

Real-time load balancing, or frequency control, is another aspect of managing variability and requires active adjustment of the load or generation to maintain a stable grid frequency and, thereby, avoid grid blackouts. The previously mentioned functionality-based categorisation is not directly applicable to this type of variation management due to differences in time-scale and procurement markets. Reserve power for frequency control is, in market-based electricity systems, procured from reserve markets rather than the day-ahead and intra-day markets in which flexibility measures to accommodate non-dispatchable generation participate. The design of reserve markets evolves over time and may differ between system operators (see, for example, the 2016 ENTSO-E survey of European system operators [16]), although efforts are being made to formulate shared grid codes and market designs [17]. In order to ensure that sufficient reserves are available to control the grid frequency, the general principle is that bids to provide reserve power will be made in reserve markets and the cheapest will be accepted until a pre-determined minimum level of supply has been reached. The accepted reserve sources are subsequently activated as needed to maintain the load balance. There are, however, technical differences between different sources of frequency reserves. Consider, for example, a biomass-fired steam turbine power plant and a reservoir-based hydropower plant. A solid fuel power plant is typically slow to adjust its power output, but once adjusted, the new output level can be maintained for a long time. In contrast, the reservoir hydropower plant has no limits to its ramping rate, except for the time that it takes for the water to flow from the reservoir to the turbine, and the speed of opening of the water gate (which if too quick can result in a so-called

'water hammer' and lead to damage [18]). However, it may not be desirable for reservoir hydropower to maintain a high output for too long, as the water in the dam is a more-limited resource. Therefore, the response to a sudden imbalance can comprise adjusted output targets from both plants, of which the hydropower plant will meet its new target well before the thermal power plant does. Thereafter, the hydropower plant can return to its original output once the slower thermal plant has reached its new target. This ordering of reserve responses is necessary due to the differences in technical properties; in some grids, these are referred to as primary, secondary and tertiary responses (referring to the speed and order of activation). More details about grid frequency control can be found in Chapter 2.

A third type of variation management can be found in the long-term planning of reservoir levels and fuel storage management, both of which can span across seasons and, to some degree, across years. Due to differences in electricity load and weather-dependent generation between years, an electricity system cannot be designed with only one weather-year in mind. The ways in which inter-annual variability affects the electricity system, as well as how this can be represented in electricity system modelling, are outlined in Section 2.3.

2.1 Electricity system modelling

Electricity system models (ESMs) have been used in numerous studies to gain insights into how electricity systems operate and are affected by various factors, such as policies, changes in costs, the roles of new technologies, and the impacts of variabilities in generation and load. ESMs are mathematical descriptions of the electricity system that, through optimisation[1], identify the optimal system operation and (possibly) the optimal composition given certain conditions and assumptions. ESMs that include investment level optimisation are often referred to as 'generation expansion planning' (GEP) or 'capacity expansion' models, with GEP being the more commonly used term[2]. Often, the objective value is the total system cost, while emissions, land use, and other aspects are included as either constraints or cost-penalties. In the realm of electricity system research, many models are employed, covering a wide span of geographical, temporal and technological scopes. Ringkjøb et al. [19], in a comprehensive review in 2018, presented the purposes, features and properties of 75 distinct and actively used energy and ESMs (although more exist). ESMs may include sector couplings and energy carriers other than electricity, although they are not designed to be as broad as *energy* system models, more often adopting a top-down perspective with broader and not-as-detailed scope. Instead, ESMs typically adopt a bottom-up approach, focusing on a higher level of detail in the technological and temporal scope, to capture the operational and dynamic interactions between technologies. The inputs to these models include techno-economic parameters (e.g., cost, efficiency, life-time) of the available technologies and fuels, a time-series of demands, hydro in-flow and non-dispatchable generation, and information about how regional nodes or grid buses are connected (if at all). If the modelling is based exclusively on new investments (to be

[1] In addition to the optimisation models described in this section, there exist electricity system simulation models. While these resemble dispatch-only optimisation models in some aspects, the way in which the solution is found is fundamentally different in the simulation models.

[2] The high number of distinct models, created by various researchers with different backgrounds and with different research aims, complicates any attempt to delineate concisely and accurately the models referred to as GEP, 'capacity expansion' or just 'electricity system model'. Long-term storage, for example, is less-prevalent in models referred to as GEP, although it still features in some models. GEP is herein used for all ESMs that involve investment optimisation.

optimised), this is sometimes referred to as *greenfield*[3] modelling. The term *brownfield* modelling is sometimes used when existing capacity is combined with new investments, and modelling with only existing capacity may be referred to as *dispatch-only*.

While it is common to provide the fuel costs as the expected market price, it is also possible to provide a limited amount of fuel supply (with an optional cost of extraction) as input. Through the marginal cost of the fuel supply constraint, the willingness-to-pay for fuel in the modelled system then becomes[4] an output of the model. Similarly, emissions can be limited by imposing either a price or a cap, resulting in the other term becoming a model output. When modelling multiple connected years, investment costs can either be provided for each year or a learning curve can be implemented by combining investments for each year with some technology-specific learning parameters [20]. However, while ESMs typically are linear (LP) or linear with some binary or integer variables (MIP), the endogenous learning-curve approach is non-linear (NLP), which complicates the optimisation. To limit the sizes and solution times of ESMs, there are always implicit or explicit compromises to exclude unnecessary non-linearities and to limit the temporal, geographical and technological scope.

Among the models listed by Ringkjøb et al. [19], the temporal and geographical scope of energy and ESMs vary from one year to several decades, and from individual buildings to the entire globe. Similarly, the temporal and geographical resolutions vary from microseconds to seasons or years, and from single nodes to tens or hundreds of nodes. However, despite improvements to the hardware and solver algorithm, the model must be limited in certain dimensions so as to limit the model size and, thereby, the time required to find the solution. Then, the options are reduced scope (i.e., excluding regions, time-periods or technologies) or reduced resolution (e.g., aggregating neighbouring regions or similar technologies or down-sampling the time-series of the load etc.). Considering these options, the temporal dimension has been particularly affected by recent improvements in modelling techniques. In **Papers I–IV**, the models are solved using hourly time-series, although techniques to limit the temporal detail are relevant to the methodology used in **Paper IV**.

2.1.1 Limiting the temporal detail

In a study carried out by Pfenninger [21] in 2017, ways to reduce the level of temporal detail in ESMs were identified and compared. Pfenninger has categorised the compared methods as down-sampling, clustering and heuristic selection of periods. Hoffmann et al. [22] identified a additional methods in a literature review conducted in Year 2020, also highlighting methods used to preserve especially relevant time-periods (e.g., extremes). The methods to preserve some time-periods differ when using only input data (*a priori*) or also incorporating a model output (*a posteriori*). Different methods to reduce the temporal detail are herein referred to as *time-series aggregation* (TSA) methods. Furthermore, the term *representative time-series* (RTS) is used to refer to time-series that are produced by a TSA method.

Although down-sampling may be the simplest TSA to implement, the potential gains are limited because the variability in an hourly time-series may be severely mis-represented by

[3] Although greenfield modelling is supposed to start from a clean slate, hydropower specifications may be given as an input due to the long life-time and regulations restricting investments in hydropower plants. For the same reasons, the existing inter-regional transmission capacity may be exogenously given in "greenfield" studies.

[4] Marginal costs can be an output if the objective value is the system cost, although it necessitates a model set-up that returns both primal and dual values.

down-sampled resolutions that are much shorter than 2–3 hours[5]. Instead, more-advanced TSA methods have often been used [23], [24] to decrease further the number of time-steps. Currently, the state-of-the-art methods not only include particularly important periods (as identified by Hoffmann et al. [22]), but also support both short-term and long-term storage. Two such TSA alternatives are particularly appealing in the context of this thesis: (i) aggregating consecutive time-steps that have a high level of similarity; or (ii) clustering portions (e.g., days) of the full time-series used to identify groups that can be characterised by a group-specific representative. The former is referred to as *chronological time period clustering* (CTPC; based on a hierarchical grouping algorithm described by Ward [25]), while the latter may be referred to simply as *representative days* (RDs)[6].

CTPC: Pineda & Morales [26] appears to be the oldest publication (from 2018) describing and using the CTPC algorithm in the form later referred to in other papers [27]–[30]. In brief, the CTPC algorithm recursively finds the consecutive time-steps with the smallest difference (based on an arbitrary number of parameters associated with each time-step) and merges them, increasing the weight of the merged time-step accordingly. As such, the process resembles down-sampling but it focuses the averaging on periods of low variability. The main advantages of CTPC are that minimal model modifications are required and that both short-term and long-term storage units are supported, since the chronology is preserved. Notably, Garcia-Cerezo et al. [28] have presented a modified version that they call *priority CTPC* (PCTPC). The PCTPC algorithm pre-assigns priority levels to each time-step, so as to alter the clustering process and better-represent the form and extremities of the original time-series. Although their implementation assigns priority based only on the input data (*a priori*), they have demonstrated improved performance across multiple model formulations, as compared to CTPC. To the best of my knowledge, no *a posteriori* (i.e., based on net-load extremes or other model variables) prioritisation has yet been demonstrated. There are, however, examples of CTPC being combined with RDs ([27], [29]), resulting in substantial benefits.

RDs: There are multiple ways to select RDs, the most-favoured of which is clustering [22]. In short, the process places each period (e.g., day) on scales for some pre-defined parameters (e.g., daily average load) and then identifies clusters with the highest degree of similarity. An RD is then chosen from each cluster, often from the cluster average (centroid) or the day that most closely reflects the cluster (medoid). Depending on the implementation of the RDs, operational constraints typically do not extend past the end of each RD, thereby limiting the duration of storage to 1 day (or period). To circumvent this limitation, new implementations of RDs (e.g., [31], [32]) map each non-representative day to the closest RD, thereby revealing the order in which each RD should be repeated to represent the whole year. Finally, by connecting the ends of each repeated RD, storage levels can vary between the RDs. While these repeated RDs result in an increased number of modelled time-steps, potentially restoring the original temporal resolution, only the storage equations need to be solved for the increased number of time-

[5] See, for example, Figure 6 in [91]. Figures 8 and 9 in [92] show a similar effect, albeit based on profiles for only a single city in Hungary.

[6] The terminology used in the surveyed literature varies. The term *representative period* is sometimes used to refer to RDs of unspecified period length. Herein, RD is used for simplicity, although the specific period length is of less importance.

steps[7]. A more detailed overview of the different methods used to link RDs and thereby enable long-term storage can be found in the review by Hoffmann et al. [22]. A comparison of the resulting investment level errors from different clustering methods has been carried out by Hilbers et al. [32], including both *a priori* and *a posteriori* methods.

In a study conducted by Gonzato et al. [33], RTS based on various TSA methods have been compared in terms of the mean time-series error, as well as the optimisation time, investment levels, and total system cost error when applied in a GEP model. Although the comparison includes multiple implementations of RDs that are able to represent long-term storage, only the Pineda & Morales [26] version of CTPC is included. Gonzato et al. [33] have reported that if long-term storage units are included and the full time-series cannot be used CTPC and so-called *Enhanced RD* (ERD) are both good options. Of these, CTPC is recommended only if a number of time-steps equivalent to 128 days (or more) is able to be modelled. It is worth noting that Garcia-Cerezo et al. [28] have shown that PCTPC results in a lower system cost error at 720 time-steps than CTPC does at 1,440 time-steps.

2.2 Grid frequency control

Regarding grid frequency control, there are three important aspects to consider: (i) the types of load imbalances that cause the grid frequency to deviate; (ii) the system inertia, which determines the rate of change of frequency (RoCoF) resulting from an imbalance; and (iii) the reserve power used to re-balance the load in real-time and, thereby, control the frequency. Since the frequency is a common variable across each synchronous grid, the geographical scale relevant to grid frequency control depends on the individual grid. Still, the responsibility for load balancing may be distributed separately to each country or sub-region in the synchronous grid.

2.2.1 Causes of imbalance

There are multiple reasons why an imbalance between the electricity generation and load occurs. One reason is stochastic load variations, which entails a high number of loads being continuously added and removed. The levels of reserves required to deal with these variations can either be determined by looking at the history of stochastic load imbalances in a region or estimated using heuristic formulae. In either case, the stochastic nature of the source of the imbalance, i.e., it being the aggregate effect of smaller unpredictable changes, is a key feature. As the loads continuously add up and cancel each other over time, the aggregate imbalance does not reach its maximum amplitude instantaneously. As such, only part of the reserve power used to counter-balance the load needs to have a low activation time. In Figure 1, which shows an example of variable loads and generation levels and the resulting imbalance, the stochastic variations are illustrated as seemingly random noise in the load.

Imbalances are also caused by variable renewable electricity (VRE) generators, through the variabilities included in forecasts and forecast errors. Intra-hourly (or intra-time-step) variability that occurs without affecting the forecasted energy per time-step may affect the real-time load balance and result in a demand for reserve power. On a grid-wide scale, the small but

[7] For regions with significant hydropower, repeated RDs should allow hydro inflow to be disregarded from the clustering process and instead applied in a less-altered way in the storage equations for repeated RDs. While doing so would increase the size of the model, it should allow RDs to be more-representative of non-inflow time-series.

rapid fluctuations in VRE generation arising from individual plants or farms (e.g., a cloud covering a solar PV park) are not very noticeable, whereas more-dramatic trends of increasing and decreasing generation (e.g., a large weather front entering a country) are reflected in the total VRE production of a synchronous grid. These large-scale changes can usually be forecasted, although the forecast error increases for smaller regions[8] and with longer time-horizons. Thus, day-ahead forecast errors can be mitigated using intra-day markets, allowing for some re-scheduling of generation and load. In an energy bidding market with sufficiently high time resolution, utilising intra-day forecasting and re-scheduling, the system stability impacts of both (previously) forecasted and non-forecasted variabilities are thus limited. The impacts of wind power on unit scheduling and the demand for reserves, as well as ways to limit such impacts, are discussed in greater detail in the paper of Kiviluoma et al. [34]. Although it is difficult to estimate the extents of these impacts in 10–25 years, it is certain that flexibility will be needed – partly to deal with the mis-match between the average energy per time-step[9] and the variable real-time power within the time-step, and partly to deal with the time-step-to-time-step ramping of (accurately forecasted) VRE. An effect analogous to the latter is shown in Figure 1, where the positive trend in load results in a repeating imbalance with a periodicity of one market period.

Other reasons for imbalances are unexpected faults in transmission, generation or load equipment. These types of faults occur suddenly and, thus, require inertia, fast-responding reserves, and long-duration reserves. Typically, grids are designed according to the N-1 criterion, which means that they should be able to withstand a fault in any one unit. Apart from local redundancy implications, this means that the levels of reserves required are determined by the largest active generator or DC connection to the grid, commonly referred to as the *dimensioning fault*, *reference incident* or simply N-1. It should be noted that the dimensioning fault may refer to the simultaneous loss of more than one unit in large grids. For the purpose of simplification, system operators may choose to make the dimensioning fault independent of whatever units are active at any point in time, and may instead specify a constant value based on the largest installed unit. Sudden loss of generation and the resulting imbalance are illustrated in Figure 1, where the level of generation suddenly drops in Period 4.

[8] Miettinen & Hannele [93] have compared wind generation forecast errors for 13 sub-regions in the Nordic synchronous grid with the forecast error of the entire grid, using Year 2014 forecasts. They calculate the mean absolute error (MAE) for the day-ahead forecast as 2.5% for the aggregate Nordic region, while the average for the sub-regions is 5.7%. Similarly, they find that the largest single, day-ahead error decreases from 80% to 13.5% of the installed capacity when going from sub-regions to the aggregate Nordic region. Forbes & Zampelli [94] have shown (in Year 2020) that the forecasting accuracy for Germany and Great Britain is continuously being improved, and they have demonstrated how an ARMAX (autoregressive–moving-average with exogenous inputs) model can create substantial further improvements.

[9] The term ‘time-step’ is used in the general sense here and refers to both a modelled time-step and the scheduling periods of an electricity planning market.

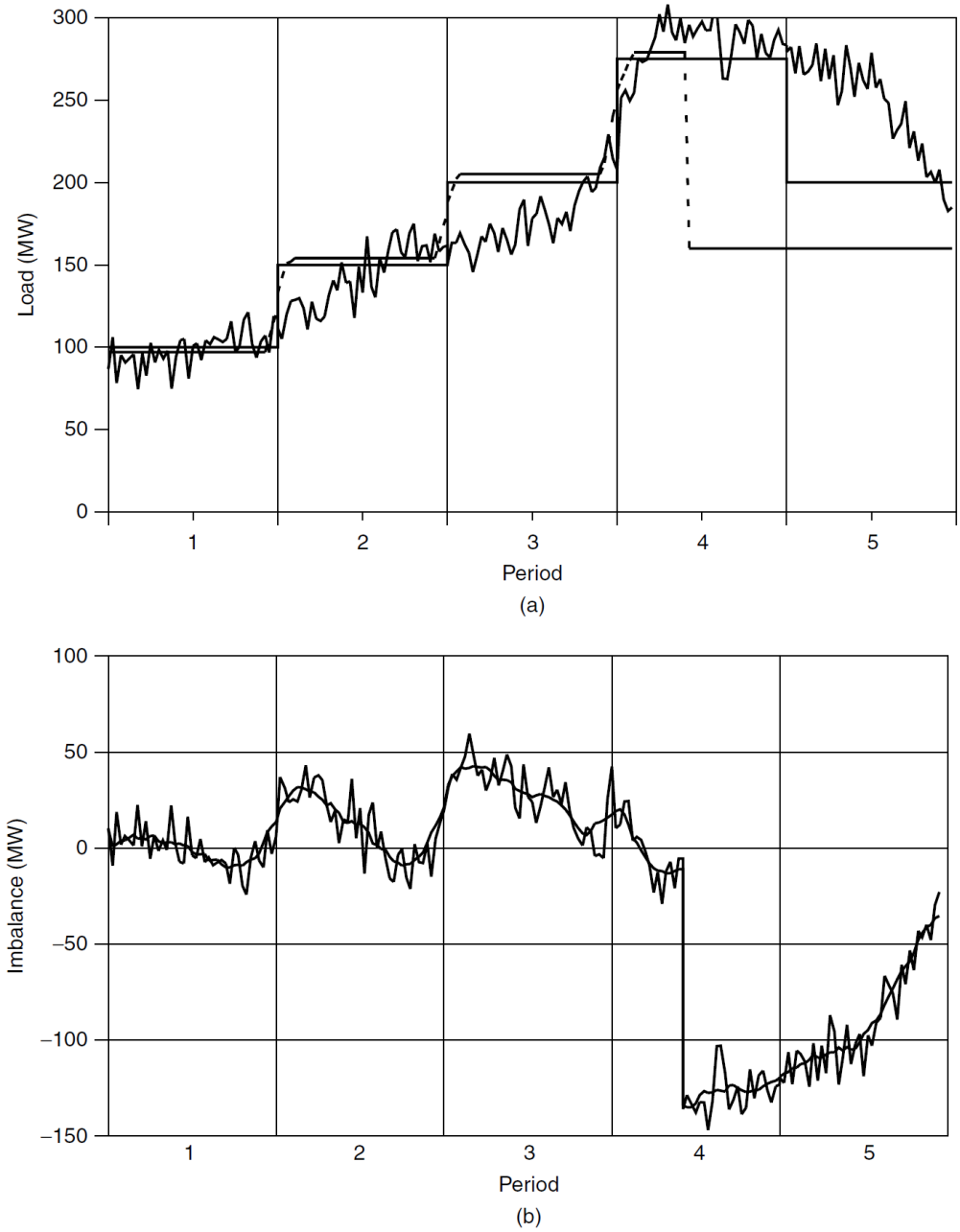

Figure 1. (a) Typical load and generation fluctuations over five market periods. (b) Imbalances resulting from these fluctuations. Figure and description are copied, with permission, from Kirschen & Strbac [35].

2.2.2 Inertia

Inertia, in the context of electrical grids, refers to the rotating masses in generators and motors connected directly to the AC frequency of the grid. Connecting to the grid without an AC/DC interface reduces the investment costs but limits the rotations per minute (RPM) to multiples of the grid AC frequency (50 Hz or 60 Hz). For example, a synchronous motor in a 50-Hz grid can run at 3,000, 6,000, ..., RPM. This means that any deviation in the grid frequency will directly affect the rotational speed of all synchronously connected machines. Thus, rapid frequency deviations can damage the equipment due to the rapid change in RPM. On the other hand, the synchronous coupling of the machines' rotational speeds to the grid frequency also

lends inertia to the grid frequency. This means that the same imbalance causes a slower frequency deviation with more inertia in place. This relationship is expressed by the so-called *Swing equation* [Eq. (1)], which gives the RoCoF, $\frac{dF}{dt}$, for any imbalance (ΔP), grid frequency (f) and system inertia constant (H):

$$\frac{dF}{dt} = \Delta P * \frac{f}{2H} \quad (1)$$

While inverter-based machines and generators do not automatically retard frequency changes, inverter-based generation can be used to ensure grid stability. The power injected by inverter-based generators can be controlled so as to follow the frequency of the grid (known as *grid-following*), while it can also set, or form, the frequency of the grid (known as *grid-forming*). However, grid-forming inverters are not an established technology in large-scale grids, and may not be necessary until there are very low levels of synchronous inertia, if ever. Due to the speed of power electronics, additional power can instead be injected in a way that simulates the effects of synchronous inertia, or in other ways that directly alleviate the imbalance (e.g., fast frequency reserves; FFR). By utilising inverter-based inertia or FFR, the amount of mechanical inertia required to maintain acceptable frequency levels can be reduced. Indeed, a shift towards inverter-based generators and less synchronous inertia may necessitate inverter-based grid support through synthetic inertia and/or FFR. Although regulations and control systems for synthetic inertia are still under development [36], [37], synthetic inertia has been employed in tests in Alberta, Canada [38]; Québec, Canada [39] and Queensland, Australia [40]. FFR, on the other hand, have already been integrated into the frequency control scheme of the Nordic grid, with approximately 300 MW of FFR being acquired in Year 2023 [41].

Although frequency control occurs on a different time-scale than the types of electricity system variations typically captured in ESMs, many studies have represented elements of frequency control in ESMs. For example, in Year 2015, during efforts to prepare the Irish grid for increasing levels of wind power, Daly et al. [42] used a unit commitment model to investigate the impacts of wind power on the inertia and RoCoF levels in the Irish grid. They used two versions of the system: a Year 2015 and a Year 2020 system with 17% and 37% of the yearly electricity supplied by wind power, respectively. They found that the demand for inertia increased fuel consumption and increased curtailment of wind power, while the impact could be largely avoided using a dynamic inertia demand (based on the generation units in operation). Johnson et al. [43] have used a similar model to study the impacts of high shares of non-synchronous generation in future scenarios (considering only nuclear power, solar PV, wind power and battery-like storage) for the Texan synchronous grid. They have reported that although different mitigation options can reduce the number of hours with critically low inertia levels, system inertia could be an obstacle to reaching 100% RE. Johnson et al. [43] concluded that changes may need to be made to the grid code, and that other technologies may be needed to provide inertia. Figures illustrating the frequency responses following a fault can be found in the paper of Tan et al. [44], in which frequency responses are simulated in scenarios with varying levels of inertia.

2.2.3 Frequency reserves

While inertia can slow down frequency changes when an imbalance occurs, re-instatement of the balance will inevitably require changes to the generation or load. This is typically achieved by increasing or decreasing the output from some generating capacity, although disconnection of the load is sometimes also used. The available reserve capacity is negotiated in a market that ensures that sufficient reserves are available to compensate for any foreseeable imbalances. The exact reserve requirements differ between grids, but following a sudden loss of generation the power must generally be replaced within seconds and remain until the cause of the imbalance is resolved. The required activation speed depends on the size of the imbalance, the system inertia, and the minimum acceptable frequency nadir.

Although the categorisations of reserves, and their respective requirements, change over time and differ between grids, there are some common terms and features. The European Network of Transmission System Operators for Electricity (ENTSO-E) often refers to frequency reserves of three categories: frequency containment reserves (FCRs); frequency restoration reserves (FRRs); and replacement reserves (RRs). After an imbalance occurs, these reserves deliver reserve power in consecutive order to contain the imbalance for as long as needed. The FCR, also known as the *primary control reserve*, is an automatic and decentralised response to arrest deviations in the frequency from the nominal value. The FRR can be automatically or manually activated by the system operator to alleviate the FCR and restore the frequency. The automatic and manual FRRs (aFRRs; mFRRs) are also known as the *secondary control reserves* and *tertiary control reserves*, respectively. Due to decreasing levels of inertia in the Nordic grid, a new type of reserve, FFR, is now used to counteract automatically (within 0.7–1.3 s) sudden changes in frequency before the FCR is expected to activate.

Not all system operators that are part of ENTSO-E use the same reserve categories or have the same requirements regarding activation time and durability. For example, the Nordic grid is not synchronous with the European continental grid and, thus, has a different dimensioning fault and reserve demand. The same goes for Great Britain, the island of Ireland, and the Baltic region (the latter being synchronous with Russia and Belarus until early 2025 [45]). However, there are clear similarities between the structures and activation times of the different reserves. ENTSO-E [46] lists the following specifications: FCR should be completely activated within 30 s and be available for at least 15 minutes, and this must be followed by aFRR, which should be fully activated within 5 minutes and also last for at least 15 minutes. mFRR, following aFRR, has a minimum activation time of 12.5 min – shorter than the previous reserves' minimum duration. In the Nordic grid, FCR-N (the -N standing for normal operation, as opposed to -D for a sudden fault in the system) should start within 30 s and be fully activated within 3 min, with the same rules for aFRR as specified by ENTSO-E. While these requirements are designed to maintain frequency stability, they are also based on the characteristics of the generators in the respective grids. Decreasing inertia levels, combined with shifting the supply of electricity, may result in changes to the current frequency control scheme, as has already happened in the Nordic grid with the introduction of FFR. Therefore, it is difficult to predict what the requirements regarding frequency reserves will look like in future scenarios based on large shares of non-dispatchable and non-synchronous sources of electricity. Nonetheless, the fundamental principles will still apply in AC electricity grids, and it will remain true that reserve power must be available to restore and retain load balance.

Using a GEP model, Van Stiphout et al. [47] have examined the impacts of FCR and FRR requirements on electricity supply investments. They have found that the impact of the reserve demand increases with the share of VRE, and that supplying reserves increases the system cost by 20%–30% at 50% RE. Considering only the supply-side reserves, they recommend that future research should include alternatives such as storage or demand-side flexibility. Battery storage is included by González-Inostroza et al. [48], as well as by Løvengreen [49], both of which studies have investigated how cost-optimised systems are affected by constraints that ensure sufficient FFR and FCR to overcome a dimensioning fault. They have both found that the reserve demand increases the total system cost by a negligible amount (0.2% in [49] and not explicitly given in [48]) when batteries are used for frequency control. Løvengreen [49] recommends future research to consider demand-side flexibility, as well as generation investments (constrained also by emissions constraints). Although some studies have included an endogenous reserve demand to compensate for forecast errors [50]–[52] or general variability [53], no GEP studies have been found to represent the flexibility required to balance the load while the non-dispatchable generation transitions from one forecasted level to the next.

The representation of frequency control implemented in **Papers I–III** features demands for inertia and reserve power availability. The reserve demand is based on N-1, stochastic load variations, and the hour-to-hour changes in wind power and solar PV generation. A more-detailed description of the implementation can be found in Section 3.2.

2.3 Inter-annual variability

Inter-annual variability plays a critical role in the planning and operation of robust and cost-efficient electricity generation systems. Variable levels of precipitation affect the availability of water for hydropower, in turn affecting the yearly energy balance, the levels of generation from run-of-river turbines, and the flexibility of systems with reservoir hydropower. Temperature variations influence the solar energy yield and the demand for energy for heating and cooling, but also evaporation which affects hydropower reservoirs. Finally, solar and wind variability obviously affects solar and wind power generation. Together, these aspects can have a drastic impact on the electricity system, giving rise to both challenging and beneficial weather-years. However, two different forms of inter-annual variability affect the electricity system: the difference in total weather-dependent generation or load per year [54]; and the difference in intra-annual[10] variability between years. These two forms each influence several aspects of the electricity system, including the cost-optimal system composition, levels of fuel consumption, electricity prices and system cost.

The transition away from fossil fuels, both in the electricity system and other sectors, increases the importance of understanding how the electricity system operates. In particular, variations in the cost of generating electricity and the demand for biofuels for electricity generation will affect both the electrified and bio-based energy sectors. To represent accurately weather-dependent generation and loads, and thereby the design and operation of the electricity system, both intra-daily variability and inter-annual variability are important [21], [55]–[57]. Fortunately, decades of hourly weather data may not be needed in GEP models if smaller, representative sets of weather data can be identified. This can be done either by applying

[10] For example, 2 years with the same total wind power generation can benefit in very different ways from added flexibility depending on how the generation is distributed over the year.

aggregation methods (such as PCTPC or RDs) to multi-decadal time-series or by finding a few weighted weather-years (or seasons) that can be combined to form a representative set. However, it is difficult to validate candidate time-series as representative unless they are applied in a GEP model and compared to a reference case with a sufficient number of simultaneously modelled weather-years. In addition, research aimed at analysing inter-annual differences in electricity system operation requires both the multi-decade investment levels and the operational data for each individual weather-year. Therefore, the input time-series used should depend on the research question. In any case, modern TSA methods allow for very low errors[11] if moderate performance improvements (50%–90% fewer time-steps) are sufficient and full resolution is not strictly necessary.

In **Paper IV**, the loads and VRE time-series are considered for the period of 1980–2019 with an hourly resolution for individual weather-years and a tri-hourly (down-sampled) resolution for all weather-years modelled simultaneously. More information about the applied methodology is provided in Chapter 3.

[11] Hoffman et al. [29] have demonstrated a method to reduce the number of time-steps (using combinations of fewer RDs and more CTPC), while minimising the incurred error. Garcia-Cerezo et al. [28] have highlighted an example with 1.6% system cost error that uses only 720 aggregated time-steps.

3. METHODOLOGY

To investigate the impacts of grid frequency control and inter-annual variability on the cost-optimal electricity system design and operation, the tools used must include endogenous investment decisions. The variability of weather-dependent load and generation must also be represented, to allow capture of the dynamics between variable renewable electricity (VRE) and flexibility measures. This chapter summarises, in Sections 3.1 and 3.2, the features of the applied generation expansion planning (GEP) models, as well as how frequency control (FC) and inter-annual variability are implemented. In **Paper IV**, a novel method for comparing weather-years is used, both to identify weather-years with particularly challenging net-load events and to incorporate them into an algorithm to identify representative sub-sets of weather-years (for the period of 1980–2019). The methods used to compare the net-loads of different weather-years, as well as the algorithm, are explained in Section 3.3.

3.1 Electricity system models

In this work, linear cost-minimising modelling with hourly time resolution is applied to a mix of individual, isolated regions (in **Paper I**), as well as to multiple, inter-connected regions (**Papers II–IV**). The models, which are written in *GAMS*, feature batteries and hydrogen rock-cavern storage (including optional fuel cells), multiple thermal power technologies, and multiple options for wind power and solar PV in each region, so as to represent a diversity of investment options. An overview of the various model features used in the modelling applied in the four papers is presented in Table 1. Two different models were used: ENODE and Multinode. In brief, ENODE is a single-region, linear dispatch and investment model with high temporal and technological resolutions. Multinode is based on ENODE and is expanded to support multiple regions and years. While the normalised time-series used as input (i.e., the profile-year) are based on historic weather-years, other inputs, such as costs and annual demand, use projections or estimates for the modelled year. The regional scopes, as defined in **Papers II** and **III** and in **Paper IV**, are shown in the maps in Figure 3 and Figure 4, respectively. To determine the profiles and potential investments for each wind and PV site, the suitable[12] land area in each region is divided into smaller cells (ca. 1-by-1 km squares) and categorised according to yearly average production. The final profiles are aggregates of the cells in each category, and the investment limit is set according to the amount of land in each category.

[12] The suitability of each portion of land is determined using labelled GIS data, excluding areas such as nature reserves. Furthermore, it is assumed that only a fraction of the potentially available land is feasibly utilised.

Table 1. Summary of the scope and features in the modeling of each paper.

	ENODE	Multinode		
	Paper I	**Paper II**	**Paper III**	**Paper IV**
Regional scope	*IE, HU, ES3, SE2*	*Brit, Iberia, Nordic*	*Brit, Iberia, Nordic*	*Nordic+*
Modelled year	2050	2020, 2025, 2030, 2040	2020, 2025, 2030, 2040	2050
Profile-year	2012	2012	2012	1980 – 2019*
Timesteps	8784	8784	8784	8760 – 113 880*
Frequency control	Yes	Yes	Yes	No
# connected regions	1	3-5	3-5	5
Heating sector	No	Yes	Yes	Yes
Electrified industry	No	H2 demand only	H2 demand only	Yes
Electric vehicles	No	Yes	Yes	Yes
GHG emissions	Zero	Taxed	Taxed	Zero
Multiple wind and PV sites	Wind only	Yes	Yes	Yes

*Multiple combinations of profile-years are applied, including one case with 39 available profile years at tri-hourly resolution.

Both the ENODE and Multinode models apply a linearised unit commitment approximation. This implementation allows for the inclusion of start-up and part-load costs, as well as part-load emissions, as described in detail by Göransson et al. [58] and based on a book by C. Weber [59]. When inter-connected regions are modelled, only the inter-regional net transfer capacity limits the electricity exchange (as opposed to using AC or DC power flow constraints). Transmission capacity between regions is exogenously set as the sum of the real transmission capacity and the cost-efficient additional capacity, as identified by ENTSO-E [60].

3.1.1 ENODE

In **Paper I**, a single-node model with hourly time-resolution and a time-horizon of 1 year is used and extended to investigate inertia and frequency reserves (FR) in VRE-dominated electricity systems. The model minimises the total cost (annualised investment and operational costs) to meet the demand for electricity in one region at a time. No inter-regional or intra-regional transmission is modelled. The model is used to study the impacts of, and interactions between, strategies and technologies to manage variations in highly decarbonised future scenarios. As such, it features high technological and temporal resolutions. A mathematical formulation of the model can be found elsewhere [58]; with additions regarding the flexibility measures described in [14]. For **Paper I**, several equations, variables and parameters are added to capture the demand and supply of FR and inertia (detailed in Section 3.2). The model is applied to four isolated regions: southern Sweden; Hungary; Ireland; and central Spain. Hydropower is made available to the Swedish region with exogenously given power and storage capacities, as well as an hourly in-flow profile. Otherwise, the regions are modelled as greenfield cases.

3.1.2 Multinode

In **Papers II–IV**, the ENODE model is developed further into the Multinode model, allowing for multiple inter-connected regions, multiple sequentially modelled years (**Papers II** and **III**), and multiple simultaneously modelled profile-years with weights representing the probability of their occurrence (**Paper IV**). For the sequential modelling of years, a *Python* script is designed to read the results of one model-run and forward the investments levels as pre-existing capacity to the next model-run. A visualisation of how the *Python* script interacts with the Multinode model is shown in Figure 2.

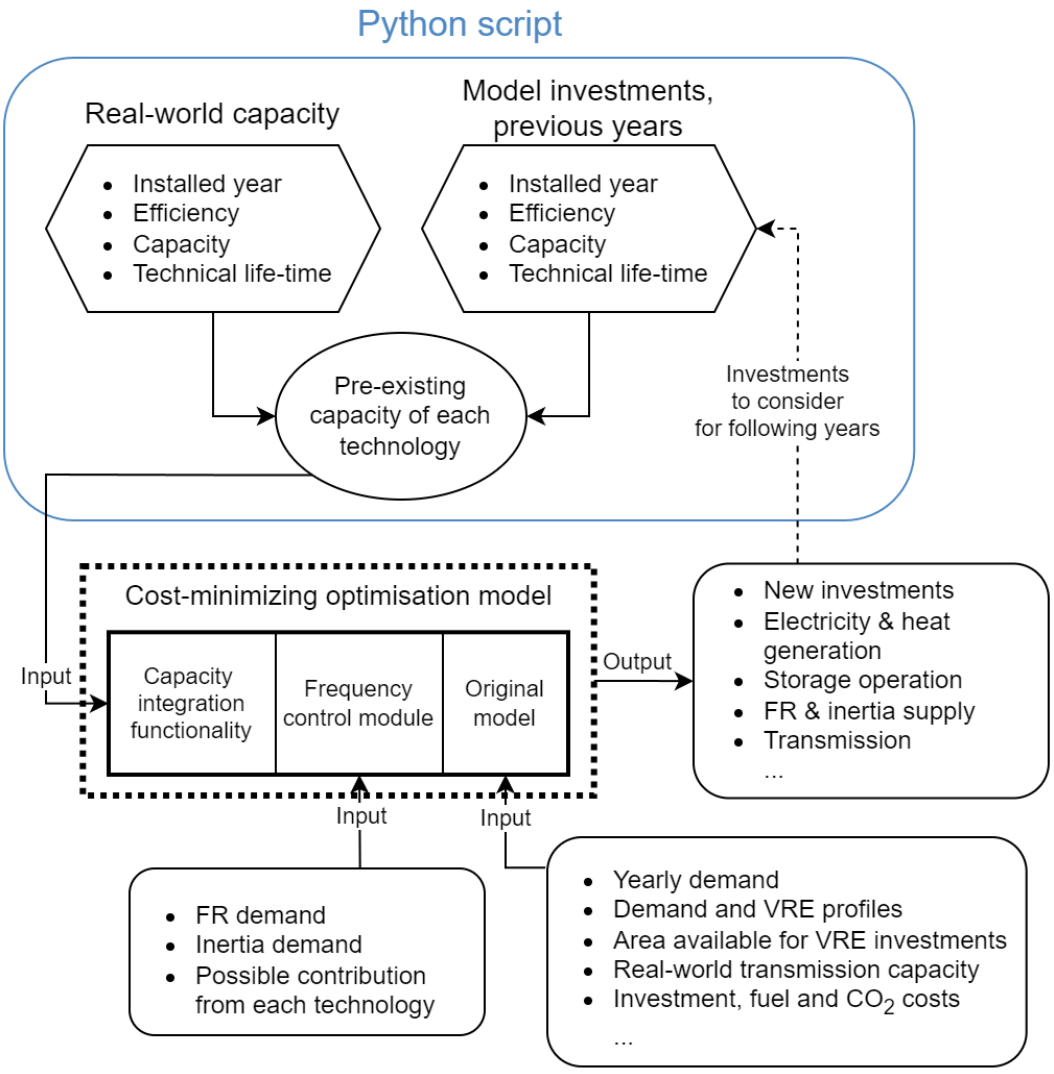

Figure 2. Illustration of the interactions between the Multinode model and the *Python* script used to determine the pre-existing capacities in **Papers II** and **III**.

By applying the *Python*-Multinode set-up to the modelled years of 2020 (dispatch-only, except peak-power investments to prevent infeasibility), 2025 (limited additional development of wind and solar power), 2030, and 2040, a transitioning electricity system is modelled for **Papers II** and **III**. It should be noted that this set-up is not designed to produce an accurate representation of the real-world electricity system transition for the modelled years. Instead, the set-up allows for comparisons of the cost-optimal capacity mix, at different time-points in the transition, for different scenarios. In this context, the years 2025, 2030 and 2040 are referred

to as the near-, mid- and long-term future time-points. Specifically, **Papers II** and **III** use the set-up to investigate how demands for FR and inertia affect the cost-optimal investment levels along an electricity system transition. This is done for three regional cases (the British Isles, the Iberian Peninsula, and the Scandinavian countries plus Finland, Netherlands and north-eastern Germany), each featuring three to five sub-regions that are connected by limited transmission capacity. These three regional cases are illustrated in the map shown in Figure 3.

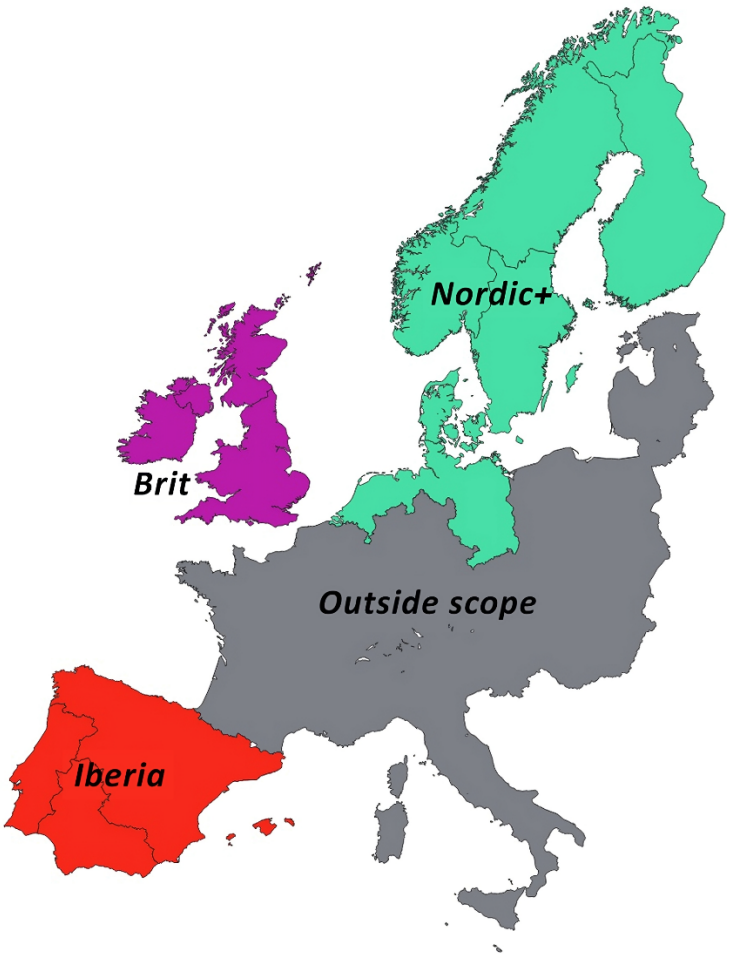

Figure 3. Map illustrating the three regional cases applied in **Papers II** and **III** with respect to existing generation and transmission capacities, VRE potentials and generation profiles, and electricity loads and load profiles. Brit: England plus Wales, Scotland, Northern Ireland, and Ireland; Iberia: north-eastern Spain, south-western Spain, and Portugal; Nordic: Finland, northern Sweden + northern Norway, southern Norway, southern Sweden + eastern Denmark, and Netherlands + western Denmark + north-eastern Germany.

For the simultaneously optimised weather-years in **Paper IV**, another set is added to the operational variables and constraints in the model. As such, the model solution features a single set of investments and the operation for each profile-year. The profile-years are not operationally linked, which means that no energy can be transferred between the years using storage systems. The consumption of biofuel can, however, vary between years, since the production and storage of biofuels are not modelled. The model set-up for **Paper IV** features six inter-connected regions, comprising Sweden, Finland, Norway, Denmark, Germany and The Netherlands, as illustrated in Figure 4.

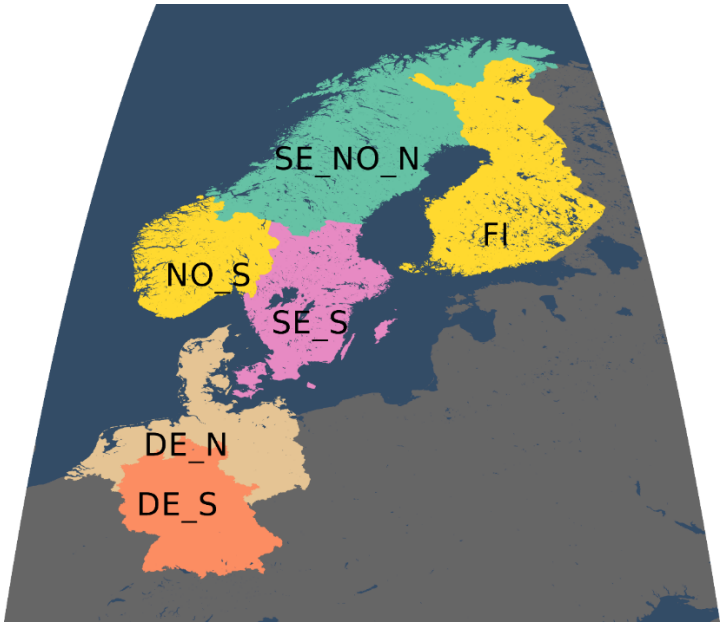

Figure 4. Map showing the geographical scope and level of resolution of this study. Note that some regions (SE_S and DE_N) include countries that are not included in the region label.

In addition to the traditional electricity demand (scaled to the projected population and efficiency increases in the modelled year), the Multinode model features non-traditional electricity demands (Table 1). Hourly demand profiles are used for electrified heating and electrified transportation systems, and a uniform demand is used to account for the electricity and hydrogen demands of the electrified industries. The yearly total loads are listed in Table 2, and the profiles are publicly available [61]. While the industry demands are evenly spread across all hours of the year, the use of batteries and hydrogen storage units can disconnect the generation of electricity from the consumption of electricity. In term of the heating demand, it is assumed that district heating networks will deliver the same amounts of heat as they do today. The remaining fossil-based share of the heating demand is assumed to be electrified (using heat pumps that produce three units of heat per unit of electricity consumed). The implementation of the electrified transport sector is based on a previous model implementation by Taljegard et al. [62], including both electricity and hydrogen demands to replace the fossil fuels. This implementation uses an aggregated representation of the vehicle fleet and assumes that 30% of the electric car fleet is charged strategically (included in the optimisation), while the remainder of the fleet charges when the cars arrive home.

Table 2. Electricity and hydrogen demands (separated by a forward slash) for each sector and industry considered in the Multinode model. For heating, the total energy demand (including the already electrified portion) is listed.

				Industry			
	Traditional load	**Heating**	**Transport [62]**	**Steel + iron [63]**	**Cement †**	**Ammonia †**	**Battery production [64]**
SE_NO_N	41.3	15.0	4.1 / 2.1	1.8 / 31.7	1.2	0.0 / 0.5	3.8
NO_S	150.5	43.3	12.2 / 7.2	0 / 0	1.2	0.2 / 2.5	5.4
SE_S	201.6	92.5	23.7 / 9.9	1.4 / 16.9	3.3	0 / 0	2.3
FI	117.2	63.6	22.3 / 13.9	2.1 / 4.4	1.5	0 / 0	1.9
DE_N	419.2	278.3	77.0 / 24.2	11.2 / 23.3	11.0	1.6 / 21.3	10.2
DE_S	566.9	443.2	127.8 / 42.1	18.6 / 38.7	26.3	1.2 / 15.5	13.0
				Conversion factors [kWh/kg]			
				0.82 / 1.7	0.96 / 0	0.45 / 5.98	47.23* / 0

†Production is assumed to remain at current levels.
*kWh of electricity consumed per kWh of battery capacity produced.

The demand and wind and solar power profiles used in this work are based on ERA5 re-analysis data [65], and generated using publicly available *Julia* scripts [66] developed for a study by Mattsson et al. [67]. This method uses machine learning to synthesise demand profiles for years and regions for which the measured demand is missing but for which data regarding the temperatures, wind levels and solar irradiation levels are available. For this work, the training for electricity demand is performed on the demand profiles for 44 regions during Year 2015, and the training for heating demand is performed on the demand profiles for 28 European regions during the period of 2008–2015. However, the high and low peaks tend to be under-estimated using this approach. This can be seen for the synthetic electricity load when analysed in isolation, albeit to a much lesser degree when combined with additional demand for electrified heating (which is highly temperature-dependent). It should also be noted that the profiles only capture already existing demand patterns, which means that they can only represent traditional loads. The settings used in the creation of the profiles for this work have been made publicly accessible along with the profiles [61].

3.2 Frequency control implementation

Rather than using the ENTSO-E reserve categories described in Section 2, the representation of frequency control implemented in **Papers I–III** uses a novel approach to FR. This is to facilitate a representation that is closer to the technical requirements and possibilities, rather than representing the current market structure in a particular region. To implement FR and inertia constraints in electricity system models, the demands for FR and inertia must be quantified and the potential for each technology to contribute must be specified. The amount

of inertia required is determined using the dimensioning fault and the highest acceptable rate of change of frequency (RoCoF). The dimensioning fault, being the largest power plant block or DC connection point, would ideally be implemented so as to depend, in each time-step, on the discrete units in operation. As this would require integer variables, thereby increasing significantly the computational load, the options are instead to make the dimensioning fault either a pre-determined constant for each region and year or in some linear way dependent upon investments and/or operation. Due to the inherently integer nature of N-1, a suitable linear implementation could not be found, so the dimensioning faults are instead assumed to be constant. The dimensioning faults are listed in Table 3 and are divided among the sub-regions according to their yearly electricity loads compared to the total electricity loads of the respective synchronous grids. In the Nordic synchronous grid, the dimensioning fault is assumed to be 1,650 MW, which corresponds to the output capacity of the Olkiluoto 3 nuclear reactor in Finland. In the continental European grid, the dimensioning fault is 3,000 MW, corresponding to the loss of two 1,500-MW nuclear reactors [68]. In the *Brit* case, a shared dimensioning fault of 1,000 MW is used, as if Ireland and the UK were synchronously connected.

Table 3. N-1 values used for each modelled copper-plate region. The green, pink and orange cells indicate the *Nordic*, *Brit*, and *Iberia* cases, respectively. A map of the modelled regions can be found in Figure 3.

Region	**SE + NO N**	**SE S**	**NO S**	**FI**	**DE N**	**UK 1**	**UK 2**	**UK 3**	**IE**	**ES N**	**ES S**	**PT**
N-1 [GW]	0.08	0.40	0.48	0.37	0.14	0.83	0.08	0.02	0.08	0.16	0.06	0.06

The highest acceptable RoCoF is assumed to be 1.5 Hz/s [proposed by ENTSO-E (2017) as the limit for windows of 1 s][13], which is used in Eq. (1) together with the inertia constant H to calculate the increased power output from all synchronous generators. Both the inertia constants and the resulting increased power outputs are listed in Table 4, which also includes synchronous condensers that are available for investment in order to provide additional inertia. Batteries are assumed to be able to deliver synthetic inertia[14] in some scenarios, limited only by their storage levels and available discharge capacities. It is also assumed that wind power can be controlled so as to contribute with synthetic inertia corresponding to an additional 13% of its output, based on the work of Imgart & Chen (2019). The combined inertial power response from all sources must then, for each sub-region, meet the N-1 values listed in Table 3.

[13] With an assumed RoCoF of 1.5 Hz/s, following a dimensioning fault, FR might be needed before 1 s has elapsed. Considering that electric boilers, batteries and curtailed solar PV all contribute to the initial FR response, activation may be initiated before 1 s, if needed.

[14] With the frequency control implementation used herein, there is no functional difference between synthetic inertia and FFR.

Table 4. Inertia constants and inertial power responses for the different synchronous generator types included in this work.

	Nuclear power	Other thermal	Hydro power	Synchronous condensers	Wind power
H [s]	6	4	3	6	-
ΔP [%]	48	32	24	48	13

As described in Sub-section 2.2.1, sudden faults (N-1), stochastic load variations, and ramping of VRE all give rise to a demand for FR. Although there can be additional needs for FR, such as forecasting errors, the demand for FR is assumed to be an additive combination of the aforementioned three sources. It is assumed that down-wards FR can always be supplied at no additional system cost (either by charging storage units or by curtailing VRE). Therefore, only up-wards FR are modelled. The FR required to compensate for ramping VRE ($R_{r,t}^{VRE}$) are approximated, according to Eq. (2), using the difference in expected output from each VRE technology for each consecutive time-step in each sub-region. In Eq. (2), i_g is the investment level for technology g and $P_{g,r,t}$ is the normalised generation profile for technology g during time-step t in region r. For the stochastic load variations, rather than extrapolating from historic data, the FR demand is estimated using a heuristic formula from the UCTE Operational Handbook [Eq. (3)]. For some empirically established parameters A and B (applied as 10 MW and 150 MW, respectively), this equation takes the peak load $L_{r,d}^{max}$ for day d and region r to calculate the FR demand as $R_{r,d}^{SLV}$. The load considered for $L_{r,d}^{max}$ does not include any sector couplings or other non-traditional electricity loads.

$$R_{r,t}^{VRE} = \sum_{g \in VRE} i_g * \max\left(P_{g,r,t} - P_{g,r,t+1} \left| P_{g,r,t} - P_{g,r,t-1} \right| 0\right) \quad (2)$$

$$R_{r,d}^{SLV} = \sqrt{A * L_{r,d}^{max} + B^2} - B \quad (3)$$

In Sub-section 2.2.1, it is also highlighted how different sources of FR demand have different requirements regarding activation speed, depending on the speed with which the imbalance occurs. While the dimensioning fault necessarily appears suddenly, both the stochastic load variations and ramping VRE are slower and are assumed to follow the rates listed in Table 5. The intra-hourly intervals (periods) listed in Table 5 are based approximately on the properties of the different sources and demands for FR, with higher resolution of the intervals at the beginning when ramping rates limit thermal power plants. The intervals combine to cover fully each hour (minus 1 s), for which time reserves corresponding to at least the reserve demand must be available. The first and shortest interval, at 1–5 s, is assumed to be the first one to act after the inertial power response and it is only needed in case of sudden faults, as indicated by a non-zero only in the N-1 row. In subsequent intervals, the stochastic load variations are assumed to start demanding FR following the equation for a first-order response, $1 - e^{-1/\tau}$, with a time constant (τ) of 60. For VRE ramping, the need for reserve power can be anticipated, to some degree, and thus the fastest three intervals are excluded to limit the required activation speed.

Table 5. Share of each reserve demand source active in each intra-hourly interval.

	1–5 s	5–30 s	30 s–5 min	5–15 min	15–30 min	30–60 min
N-1	1	1	1	1	1	1
VRE ramping	0	0	0[15]	1	1	1
Stochastic load variations	0	0.08	0.39	0.99	1	1

A simplified version of how FR is supplied is visualised in Figure 5, which shows how storage systems, thermal power plants, power-to-heat plants, VRE and transmission among neighbours contribute to the total FR supply. Batteries and hydrogen storage units are limited both by their storage levels and their unused discharge capacities. For storage units that are being charged, the potential reserve contribution corresponds to the sum of the charging rate and the unused discharge capacity, though still limited by the storage level. Thermal power plants can contribute according to their ramping rates. However, only capacity that is operated at part-load can contribute without being limited by the start-up time. Since the model includes a part-load penalty corresponding to a loss of thermal efficiency, this contribution is associated with a system cost even though the reserve implementation requires only the *availability* of reserve power. Hydropower works in a manner similar to thermal power plants, except that there are no differences between the contributions of the part-load and off-line capacities of hydropower. Power-to-heat from heat pumps and electric boilers to district heating networks are assumed to be able to turn off within 1 s, so as to provide reserves. Any potential additional investment or maintenance cost required for such a rapid shut-down is not considered. While activation of the reserve from storage units and power-to-heat would result in an energy deficiency in the storage or heat balances, it is assumed that reserves that increase consumption (or decrease generation), which are not considered in this work, would compensate for these energy deficiencies. Lastly, any curtailed VRE generation is added to the supply of available FR. If the total supply of reserves in a sub-region exceeds the demand and there is unused transmission capacity, it is assumed that the excess reserves can be exported. The precise constraints governing the supply are detailed in the mathematical description of the model in **Paper II.**

[15] In **Paper II**, it was erroneously stated that VRE ramping is assumed to require reserves with an activation time of 30 s. Instead, the results presented in **Papers II** use the values presented herein, allowing slightly slower reserves (5 min) to compensate for VRE ramping. A request for revisions has been sent to the publisher of **Paper II**.

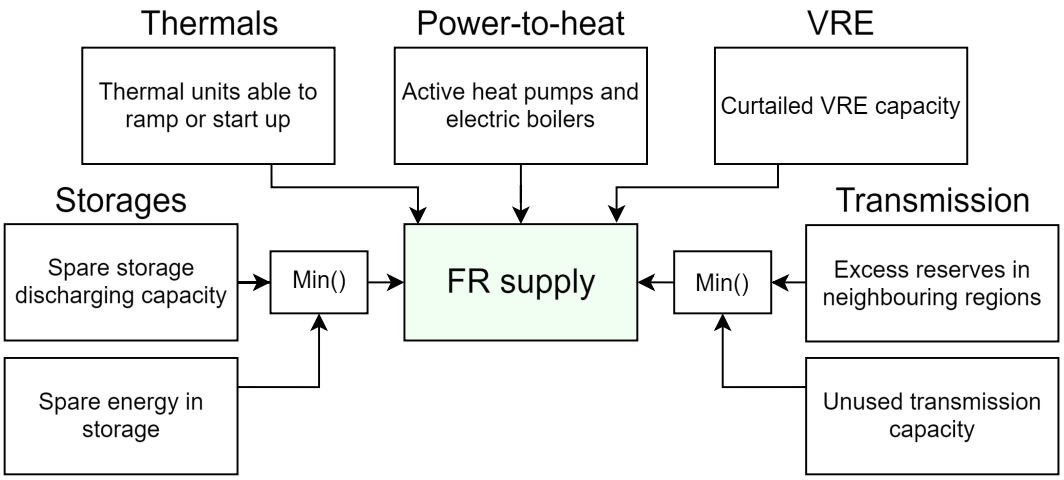

Figure 5. Simplified diagram of the various sources of FR supply. The storage systems considered in this work are batteries and hydrogen caverns.

Similar to the ways in which the demands for reserves differ between the reserve intervals, the supply to each interval varies according to the values listed in Table 6. The thermal ramping and start-up times are based on a technology catalogue issued by the Danish Energy Agency & Energinet (2017), with the exception of those for the nuclear technology, which are based on Schröder et al. (2013).

Table 6. Potential reserve availability, as a fraction of the rated power, for each technology and FR interval. For on-line thermal power plants running at part-load, the table shows the fraction of the on-line ("spinning") capacity by which the part-load can be increased.

	O_1^{dur} 1–5 s	O_2^{dur} 5–30 s	O_3^{dur} 30 s– 5 min	O_4^{dur} 5–15 min	O_5^{dur} 15–30 min	O_6^{dur} 30–60 min
Power-to-heat	1	1	1	1	1	1
Curtailed VRE	1	1	1	1	1	1
Energy storage units						
Li-ion battery	1	1	1	1	1	1
Hydrogen	1	1	1	1	1	1
Flywheels	1	1	1	1	1	1
Hydropower	0	0.15	0.3	1	1	1
On-line thermal plants						
CCGT	0	0.0125	0.075	0.75	1	1
OCGT	0	0.1	0.3	1	1	1
ST	0	0.025	0.05	0.2	0.6	1
Nuclear	0	0	0	0.375	1	1
Off-line thermal plants						
CC GT	0	0	0	0	0	0
OC GT	0	0	0	0	1	1
ST	0	0	0	0	0	0
Nuclear	0	0	0	0	0	0

CCGT, combined-cycle gas turbine; OCGT, open cycle gas turbine; ST, steam turbine; VRE, variable renewable electricity.

3.3 Analysing and selecting weather-years

As highlighted in recent studies presenting improved time-series aggregation (TSA) methods (e.g. [31], [32], [73]), the representativeness of a time-series depends not only on the its load and weather-data, but also on the model and scenario it is applied to. Especially so for GEP models, since the resulting VRE capacity mix dictates how the time-series (i.e. VRE generation profiles) affect the net-load profile that non-VRE technologies operate within. The available flexibility measures, in turn, affect the system cost associated with a variable net-load profile. The issue, then, is that the VRE generation profiles also affect the cost-optimal capacity mix. While there are other model outputs that can be relevant for the creation of a representative time-series (RTS), such as the cost of generating electricity in each timestep or the (dis)charging of storages, these are highly correlated with the net-load. Net-load is thus the variable used to select RTS in this work. The RTS are, however, not generated using conventional TSA methods. Instead, the RTS are made up of a number of weighted weather-years (referred to as *weather-year sets*). The years are selected through an error-minimizing optimization, based on each year's net-load characteristics (further described in Subsections 3.3.1 and 3.3.2). No TSA is applied to the individual weather-years, as is discussed in Section 5.3 regarding future research.

A capacity mix, and thereby the net-load, can be found in one of three ways: (i) using an exogenous, reference capacity mix, (ii) running the GEP model once using part (or all, if possible) of the time-series, or (iii) looping the GEP model and RTS-creation process until some criteria is met. Option two, using the full time-series, should be the go-to option to ensure a true reference case. If the full time-series makes the model intractable, the next-best option may be to apply mild TSA (i.e. slightly reducing the resolution using down-sampling or PCTPC[16]). This may cause a slight misrepresentation of the short-term storage or peak thermal capacity but is unlikely to significant effect on the VRE capacity mix. In **Paper IV**, the third option (looping) is used, though validation is done against the capacity mix of the full time-series down-sampled to tri-hourly resolution. While looping does not necessarily mean that the final RTS are representative also for the full time-series, it is a likely outcome for sufficiently large RTS. For this thesis, the sets of weather-years found using option three (looping) are compared with those found using option two (capacity mix based on all weather-years). One out of the six sets with hand-picked years and two out of the three sets without hand-picked years were affected by the changed source of capacity mix. Although, as the results in Section 4.2 show, the resulting investment levels are similar.

The algorithm used to find representative sets of weather-years is described in **Paper IV** and illustrated as a flowchart in Figure 6. The net-load recurrence matrices used in step 2, as well as how they are analyzed to identify particularly challenging weather-years, are described in Subsection 3.3.1. The optimization used to find the combination of years with the smallest error (step 3) is described in Subsection 3.3.2.

[16] In Figures 9, 10, 13 & 14 in [28], Garcia-Cerezo et al. show minimal-to-no effect on solar PV and wind power investments until more than 80-90% of timesteps are aggregated.

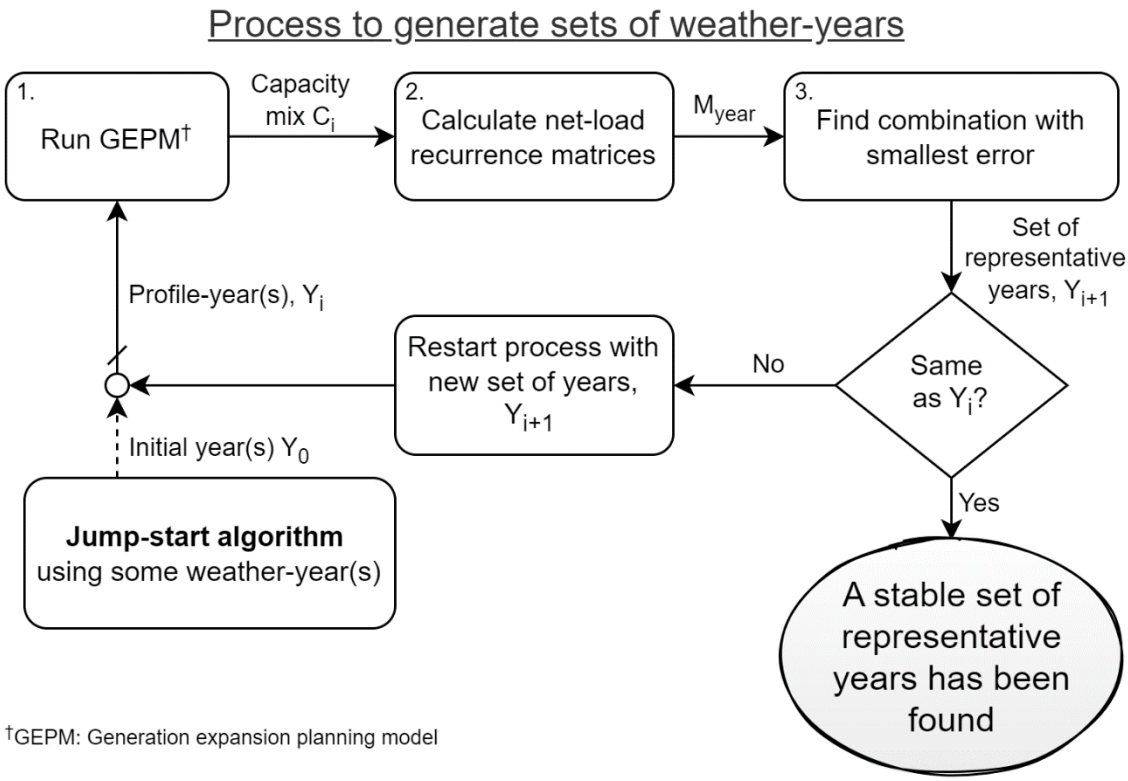

Figure 6. Flowchart illustrating the algorithm for finding a set of weather-years that represents the net-load variations in the 40-year period of 1980–2019.

3.3.1 Net-load recurrence matrix

One way to represent the net-load variability of an electricity system is to count the recurrences of net-load events for each combination of amplitude and duration. The resulting matrix can be illustrated in a heat map or used as a fingerprint of that period's net load variability. This process was originally described in a study carried out by Göransson [11] (see *Algorithm 1*), and is here modified to create a matrix that is better suited as a fingerprint. To reduce the risk that a single sunny day interrupts an otherwise high net-load period, a 12-hour rolling average is applied to the hourly net-load, thereby reducing low-energy fluctuations[17]. It is assumed that the short-duration variations (≤12 hours) are similar for all years and are not relevant in terms of the selection of representative weather years. While transmission bottle-necks between regions are accounted for in the GEP optimisation, the net-loads of all regions are aggregated when building the net-load recurrence matrix. In Figure 7, an example of the net-load recurrence matrix is illustrated as a heatmap. The net-load recurrence matrix is calculated using time-series for the entire period of 1980–2019 and a capacity mix with 66% VRE. The heatmap shows that net-load recurrence is highest for low durations and low amplitudes, with the peak net-load being around 360 GW and the longest positive net-load duration being 127 days. However, the 127-day event has a very low amplitude and can easily be covered by base-load thermal power or hydropower. In the reference system shown in Figure 7, there are approximately 32 GW of reservoir hydropower and 51 GW of nuclear power. Above this amplitude (at around 83 GW), the longest duration is 56 days and is annotated in Figure 7 as

[17] A longer rolling average horizon would better preserve the duration of net-load periods, albeit at the cost of further distorting the amplitude of the net-load peaks.

belonging to the weather-year of 2002–2003 (1st of July 2002 to 30th of June 2003). The contours of other weather-years that are on, or lie close to, the heatmap outline are also highlighted in Figure 7. All individual weather-years are considered in the summer-to-summer format (as for 2002–2003), rather than as calendar years. This is done to preserve continuity during the winter season, when long periods of energy deficiency are most likely to occur. As illustrated in the flow chart in Figure 6, once a VRE capacity mix is identified (e.g., by running the GEP model), it is used to calculate the net-load recurrence matrices in Step 2. This includes both the matrix for the entire period of 1980–2019 and the matrices for each individual weather-year. These matrices are the basis for the next step, in which the linear combination of weather-years with the least error, as compared to the 1980–2019 period, is found.

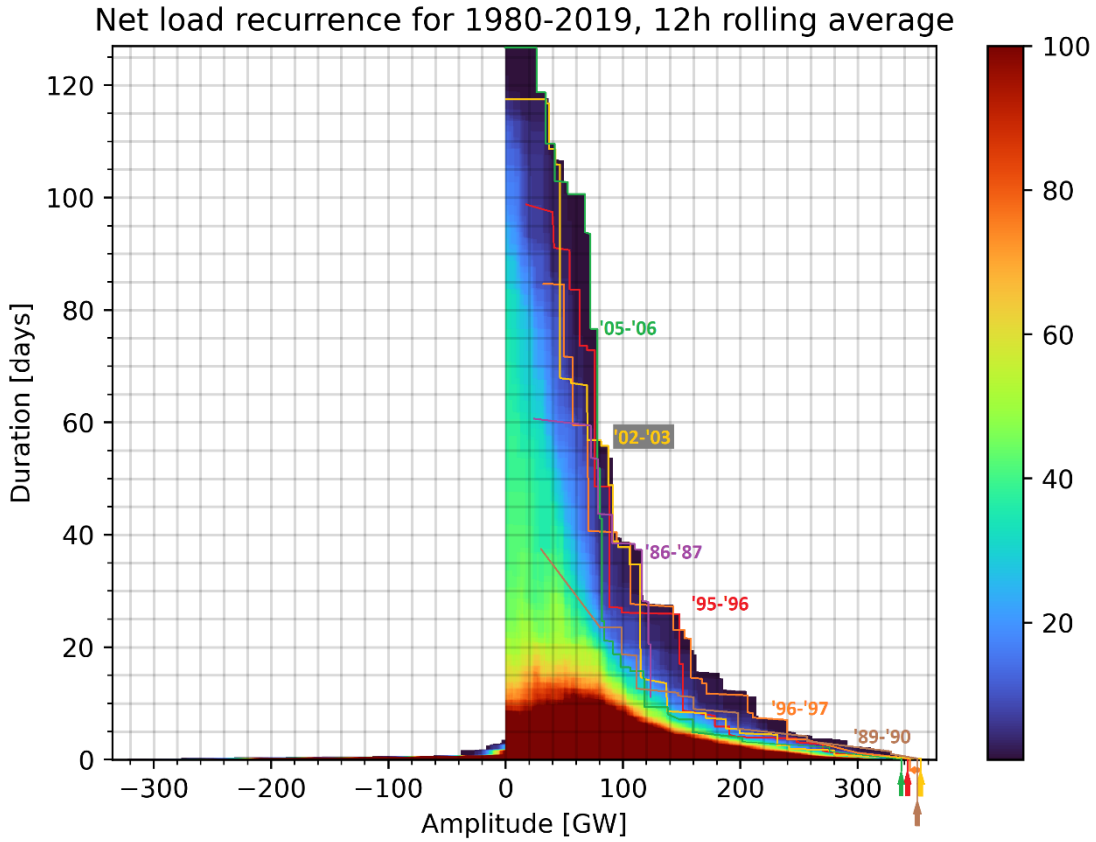

Figure 7. Heat map of the recurrence of each combination of amplitude and duration of the net-load between Year 1980 and Year 2019, for a capacity mix with 66% wind and solar power, as obtained from the modelling in this work. Years that make up the outline of the heat map are contoured and annotated (e.g., "05-06") by hand. The numbers of recurrences are capped at 100 in the heat map, to enhance clarity in the medium-to-low-recurrence regions.

From an energy system analysis point-of-view, for a set of weather-years to be representative it should include both the medium-to-high-probability periods of various seasons and the dimensioning low-probability periods. These dimensioning low-probability periods include (at least) a net-load peak and a period of high energy deficiency, considering generation from VRE, reservoir hydropower and base-load power. While it may appear straight-forward to identify the hour with the highest net-load and the year or season with the largest cumulative energy deficiency, given a capacity mix, this may not be optimal. Due to potential interactions with short-term storage systems, it is possible that the net-load peak with the highest

instantaneous amplitude does not drive capacity investments as much as, for example, the second-highest peak. Similarly, if multiple technology options (e.g., types of long-term storage or types of fuel conversion) are available for dealing with energy-deficient periods, then the choice of dimensioning period may be less straight-forward.

To cover a large span of challenging low-probability periods, the choice regarding which periods to explicitly include is, in **Paper IV**, made for whole weather-years and is based on a visual analysis of recurrence matrices. A visual analysis of Figure 7 indicates that (with 83 GW of dispatchable nuclear and hydropower) a combination of the periods of 2002–2003 and 1996–1997 would cover a large portion of the contour, including a high net-load peak. While this method allows for the inclusion of a wide range of low-probability net-load events, it does not guarantee that the dimensioning periods are included. While the rolling average reduces the impact of a single sunny day, long periods of energy deficiency may still get split into multiple, medium-duration events that are not appearing at the contour of Figure 7. The model results from weather-year sets with and without hand-picked years are, thus, compared in Section 4.2, and the method used to select dimensioning periods is discussed in Chapter 5. Regardless of whether hand-picked extreme weather-years are used, the base/normal weather-years must be selected in a different way, as described in the next sub-section.

3.3.2 Fingerprint matching

Using the *JuMP* software package in *Julia*, sets of weather-years are optimised to find the best way to combine them and represent the reference 1980–2019 recurrence matrix (m^{ref}). The optimisation problem is formulated as an MIQCP[18] as follows, where the error, e, is minimised for X number of weather-year matrices (m_y). Both the reference and yearly matrices ($m_{y,i,j}$) are of size $m \times n$.

$$e = \sum_{i=1}^{m}\sum_{j=1}^{n} {M_{i,j}^{diff}}^2 \tag{4}$$

$$M_{i,j}^{diff} = \sum_{y \in Y}\left(m_{y,i,j} * w_y\right) - \frac{m_{i,j}^{ref}}{40}, \qquad \forall\, i \in \{1,2,\dots,m\}, j \in \{1,2,\dots,n\} \tag{5}$$

$$\sum_{y \in Y} w_y = 1 \tag{6}$$

$$0 \le w_y \le x_y, \qquad \forall y \in Y \tag{7}$$

$$\sum_{y} x_y = X, \qquad x_y \in \{0,1\} \tag{8}$$

This is carried out for sets of 2–12 weather-years, both with and without hand-picked years. Hand-picking is done by locking the respective weights (w_y) to 1/40, as the probability should reflect the extreme events. In Eq. (4), each M^{diff} element is squared before summation, but it would also be possible to use absolute values or, for example, the square-root of the absolute values. Square-root (or $\log_{10}$) values may be of particular interest when no hand-picked extreme

[18] Mixed integer quadratically constrained program. The optimisation is completed in seconds or minutes for sets of only a few weather-years, although it takes several hours when 10 years of weather data are included.

years are used, as they reduce the differences between high and low values in M^{diff}. In doing so, the larger areas along the contour become more highly valued despite their low recurrence, thus giving a better representation of rare net-load events. As such, the weather-year sets generated with hand-picked years use the MIQCP formulation above (squared M^{diff} elements), while sets without hand-picked years use heuristic optimisation with the square-root of M^{diff} elements.

4. MAIN RESULTS

The main findings in **Papers I–IV** are presented here, focusing on the technologies found to be crucial for providing frequency reserves (FR), inertia and inter-annual flexibility in the modelled systems. Additional results that are of particular interest, and not described in **Papers I–IV**, are also presented.

4.1 Key technologies for frequency control supply

KEY MESSAGE. The key message from **Papers I–III** regarding grid frequency control in future electricity systems is that while frequency control and grid stability are important issues, fulfilling these technical requirements does not appear to be costly in relation to the amount of generated electricity (<0.5 €/MWh in **Paper II** once new investments are allowed). Due to their limited impacts on the total system cost, they also do not significantly affect the system composition. Although the reserve supply is a combination of technologies, batteries play a key role in limiting the system cost.

The results in **Paper I** show, for all four investigated systems (Hungary, Ireland, northern Spain and southern Sweden in Year 2050) with high shares of variable renewable electricity (VRE), that batteries play a significant role in limiting the system cost of frequency control (FC). This is achieved by providing both low-cost FR and synthetic inertia. When synthetic inertia is not allowed, mechanical inertia is supplied by the addition of synchronous condensers. **Paper II** extends the geographical scope to three larger regions (Northern Europe, the British Isles and the Iberian Peninsula) while modelling multiple consecutive years, generating results similar to those in **Paper I**. However, **Paper II** finds that the system cost of providing FC decreases significantly in the mid-to-late-term stages of the transition. In the early stages, access to batteries and curtailed VRE is limited, so additional fuel and part-load thermal costs are incurred to ensure the provision of FR. **Paper III** compares the marginal costs of the reserve and electricity demands, using the same model set-up as in **Paper II**. The combination of batteries, hydropower and high levels of VRE (none of which incur a direct cost to make reserve power available) causes the reserve market size to decrease by up to 95% in the long-term future time-point. **Paper II** also investigates scenarios with FR participation from battery electric vehicles (BEV) at no explicit cost, and shows that their participation eliminates the system cost impact of FC entirely across all regions and time-points. While many countries split the FC responsibilities (like those assumed for the dimensioning fault in **Paper II**), there are also isolated grids in which the inertia and FR demand impacts may be closer to those in **Paper I**. A notable case is the Irish grid, whose isolation means that the impact of FC may be higher than indicated by the results in **Paper II**.

The total electricity supplied per technology group for each year in each regional case, resulting from the modelling in **Paper II**, is shown in Figure 8. Clear differences are evident across the years and regions, with wind and solar power dominating all regions in the mid-term and long-

term. While there are differences in system cost between the scenarios with FC (*Full FC*) and without FC (*No FC*), driven in large part by additional battery power investments, Figure 8 illustrates the lack of impact on the electricity supply. In other words, the investigated systems transition towards carbon-neutrality along the same pathway, regardless of whether FC is considered in the model.

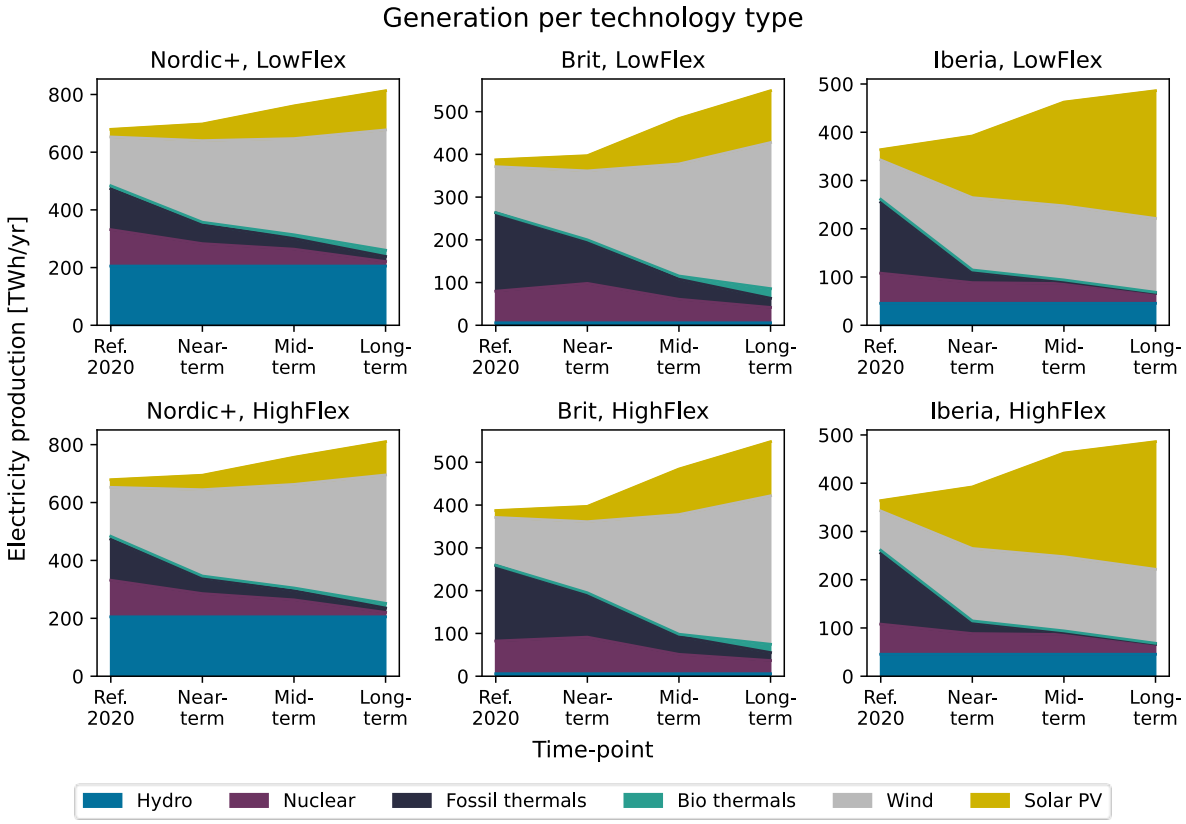

Figure 8. Yearly electricity supply development from Year 2020 to the long-term future in each geographical case in **Paper II**, without FR and inertia constraints (*No FC*), as well as with FR and inertia constraints (*Full FC)*.

The value of FR from batteries is reflected in Table 7, which shows differences in the system cost and thermal cycling cost (accumulated across the investigated years) when various technologies are excluded from the FR and inertia supply. Excluding batteries from the FC has a strong impact on the accumulated system cost, whereas the impact of excluding VRE or heat pumps and electric boilers is minor in comparison, and only found for the *Nordic* case. In the *No bat. FC* scenario, no single technology is used to replace batteries. Instead, the increased system cost arises from a combination of increased curtailment (and fuel costs), increased investments in traditional power plants, and higher power-to-heat (PtH) usage.

Table 7. Total system costs and thermal cycling costs, accumulated across all four time-points, for the technology-restricted scenarios.

	Total system cost [G€]				Thermal cycling cost [G€]			
	Full FC	*No bat. FC*	*No VRE FC*	*No PtH FC*	*Full FC*	*No bat. FC*	*No VRE FC*	*No PtH FC*
Brit	71.181	+2.99	+0.03	+0.01	0.94	+0.27	+0.00	+0.00
Iberia	44.044	+1.10	+0.00	+0.00	0.22	+0.11	+0.00	+0.00
Nordic	63.586	+3.11	+0.34	+0.73	0.10	+0.49	+0.02	+0.02

Due to the apparently large system cost savings achieved by using batteries for FR, the results for two additional scenarios are shown in Table 8. These scenarios, *No bat. double-use* and *EnergyRes,* impose additional constraints on batteries to counteract the relative advantage gained by two factors: (i) the model having perfect foresight (i.e., battery discharge can be perfectly planned); and (ii) no available reserves being activated (i.e., reserves made available from batteries do not directly[19] affect the storage balance). In the *No bat. double-use* scenario, separate battery units must be invested in to participate in the energy and FR balances, meaning that all batteries are single-purpose only from the point of investment. In the *EnergyRes* scenario, the reserves supplied by batteries lock the corresponding amount of energy in the battery for 12 hours, so as to extend the time needed to replenish the hypothetical discharged energy. It should be noted that the amount of locked-in energy accumulates if additional reserves are made available within the 12-hour window, in effect assuming that all reserves that originate from batteries are activated and only re-filled (albeit without affecting the grid electricity balance) after 12 hours. Thus, both scenarios feature constraints that are more extreme than real-world limited foresight and stochastically activated reserves.

Table 8. Total system costs, accumulated across all four time-points, for the *Full FC*, *No bat. FC*, *No bat. double-use* and *EnergyRes* scenarios.

	Total system cost [G€]			
	Full FC	*No bat. FC*	*No bat. double-use*	*Energy-Res*
Brit	71.181	+2.99	+0.41	+0.66
Iberia	44.044	+1.10	+0.43	+0.16
Nordic	63.586	+3.11	+0.38	+0.91

[19] While there is no direct effect on the storage balance from supplying reserves from batteries, there can be an indirect effect. Reserves can only be made available from batteries if there is unused discharge power and energy available for the hour in question. After this hour, it is assumed that symmetry in the demand for up- and down-regulation will allow any hypothetically used energy to be re-filled.

Table 8 shows that while the *No bat. double-use* and *EnergyRes* scenarios increase the system cost relative to the *Full FC* scenario, this increase is not as large as that seen when batteries are completely unable to provide FR. The key role assigned by the model to battery storage units is, thus, not simply an artefact of perfect foresight or of reserves not being activated. Indeed, a large share of the system value found when using batteries for FR remains, even if imposing overly strict constraints. It should be noted that when battery-based FR is allowed, the generation outputs from thermal power and hydropower are occasionally adapted to provide indirect FR. **Paper II** finds that by increasing or shifting the generation from dispatchable generation, the otherwise used battery capacity can instead be made available for FR. In addition, the avoided battery discharge can displace future dispatchable generation and avoid increases in fuel consumption.

4.2 Representative weather-year sets

KEY MESSAGE. In **Paper IV**, it is found that there are large differences in the resulting system compositions when using individual weather-years in the Multinode model. This difference is noted also between "normal" weather-years with average hydro inflow and wind full-load hours. On the other hand, weather-year sets generated using the algorithm proposed in **Paper IV** show small differences in terms of the resulting system composition. Modelling using a combination of as few as 3 years is found to improve significantly the similarity of technology investments to those found when modelling all 39 years, as compared to modelling "normal" or extreme single years.

The weather-year sets found and evaluated in **Paper IV** are generated using the set-finding algorithm (detailed in Section 3.3) in an iterative fashion, to identify sets that are self-representative of the capacity mix in which they result when modelled. As previously mentioned, an alternative approach to finding sets of weather-years can be used if a solution can be found when modelling all weather-years (*All years*). In that case, the capacity mix from *All years* can be used as an input to the algorithm without iterating. The resulting set of years may not be representative of their own net-load characteristics (as the sets from **Paper IV** are), but they would be the most-representative sets of weather-years for the full period of weather-years. Such weather-year sets (directly based on *All years*), with varying sizes, are presented in Table 9. In Table 9, seven sets of weather-years including hand-picked years are presented along with five sets of all-optimised weather-years. The hand-picked years are, where applicable, 1996–1997 and 2002–2003 (for the sake of brevity, not included in the table).

Among the weather-year sets with hand-picked years listed in Table 9, only *2 HP + 3 opt.* differs from the sets found in **Paper IV**. However, all but one (*2 opt.*) of the weather-years sets without hand-picked years differ from those found in **Paper IV**. This indicates that the algorithm is more robust to the choice of process to find the reference capacity mix when hand-picked years are included.

Table 9. Seven weather-year sets, including 1996–1997 and 2002–2003 as hand-picked years (not listed in the table), followed by five weather-year sets with only years found through optimisation. The sets are generated using the capacity mix of *All years*.

2 HP + 1 opt.	Years	2001–2002					
	Weights	0.950					
2 HP + 2 opt.	Years	2000–2001	2016–2017				
	Weights	0.359	0.591				
2 HP + 3 opt.	Years	1990–1991	2009–2010	2015–2016			
	Weights	0.260	0.318	0.372			
2 HP + 4 opt.	Years	1990–1991	1994–1995	2008–2009	2015–2016		
	Weights	0.245	0.210	0.253	0.242		
2 HP + 5 opt.	Years	1993–1994	2000–2001	2003–2004	2010–2011	2011–2012	
	Weights	0.138	0.180	0.202	0.232	0.198	
2 HP + 6 opt.	Years	1993–1994	1999 – 2000	2000–2001	2003–2004	2010–2011	2011–2012
	Weights	0.121	0.117	0.175	0.202	0.186	0.149
2 HP + 10 opt.	Years	1981–1982	1986–1987	1988–1989	1990–1991	1998–1999	2008–2009
	Weights	0.105	0.09	0.092	0.104	0.086	0.086
	Years	2014–2015	2015–2016	2017–2018	2018–2019		
	Weights	0.078	0.127	0.088	0.094		
2 opt.	Years	2000–2001	2016–2017				
	Weights	0.392	0.608				
3 opt.	Years	1981–1982	2014–2015	2016–2017			
	Weights	0.275	0.335	0.390			
4 opt.	Years	2000–2001	2002–2003	2014–2015	2016–2017		
	Weights	0.250	0.200	0.259	0.291		
5 opt.	Years	1982–1983	1997–1998	2002–2003	2004–2005	2009–2010	
	Weights	0.201	0.157	0.175	0.265	0.202	
6 opt.	Years	1983–1984	1992–1993	1994–1995	2001–2002	2009–2010	2012–2013
	Weights	0.184	0.184	0.190	0.166	0.150	0.126

Paper IV finds that when the weather-year sets are applied in the GEP model, the resulting capacity mixes largely resemble each other and *All years*. The greatest difference between the sets and *All years* is a general lack of peak thermal capacity[20], although the capacity is larger than for most individually modelled years. Between the sets of weather-years, the largest difference found is an increased peak thermal capacity for the sets with four optimised years (due to 1994–1995, a dimensioning peak year, being included by chance). No clear difference is found in **Paper IV** between the weather-year sets with and without hand-picked years.

In Figure 9, the capacity mixes of the weather-year sets listed in Table 9 are shown, together with the capacity mix of *All years*. For the first five sets (without hand-picked years), Figure 9 shows an overall improvement in representation for many of the technologies as the number of years in the weather-year sets increases. While the capacity mix of the largest all-optimised set (*6 opt.*) is very close to that of *All years* for all other technologies, the amount of solar PV capacity is under-represented by 44 GW (7.5%). A similar under-representation of solar PV is seen for almost all the weather-year sets. For the sets with hand-picked years, no clear trend is observed as the number of years in the weather-year sets increases. Furthermore, if comparing the sets with and without hand-picked years in Figure 9 it is difficult to conclude that one group of sets clearly offers better representation of *All years*. The difference is, however, greater than that seen in **Paper IV** using the iterative method. The excessive amounts of nuclear power noted for the *3 opt., 4 opt.* and *5 opt.* sets (compared to the *2 HP + 1 opt., 2 HP + 2 opt.* and *2 HP + 3 opt.* sets) suggest that hand-picked years are useful when five or fewer weather-years are included. Although *6 opt.* offers better representation than the large sets with hand-picked years, it is difficult to ascertain a trend in the absence of more all-optimised sets[21]. Furthermore, the largest set, *2 HP + 10 opt.*, does not appear to give a capacity mix closer to *All years* than either *2 HP + 5 opt.* or *2 HP + 6 opt.*, which suggests that there is little value in including more than four or five optimised weather-years in a set that includes hand-picked years.

[20] The 12-hour rolling average in the net-load recurrence matrix is expected to hide the dimensioning hour for peak thermal power. A better capacity mix may be achieved by hand-picking the weather-year (or day/week) with the highest actual net-load. While imposing a minimum level of dispatchable power may achieve the same effect, it is not obvious how to represent the contribution of short-term storage (e.g., battery) under such a constraint.

[21] Prohibitive computational times when not using the MIQCP model formulation (recall the error summation method from Sub-section 3.3.2) prevented the discovery of any larger all-optimised sets.

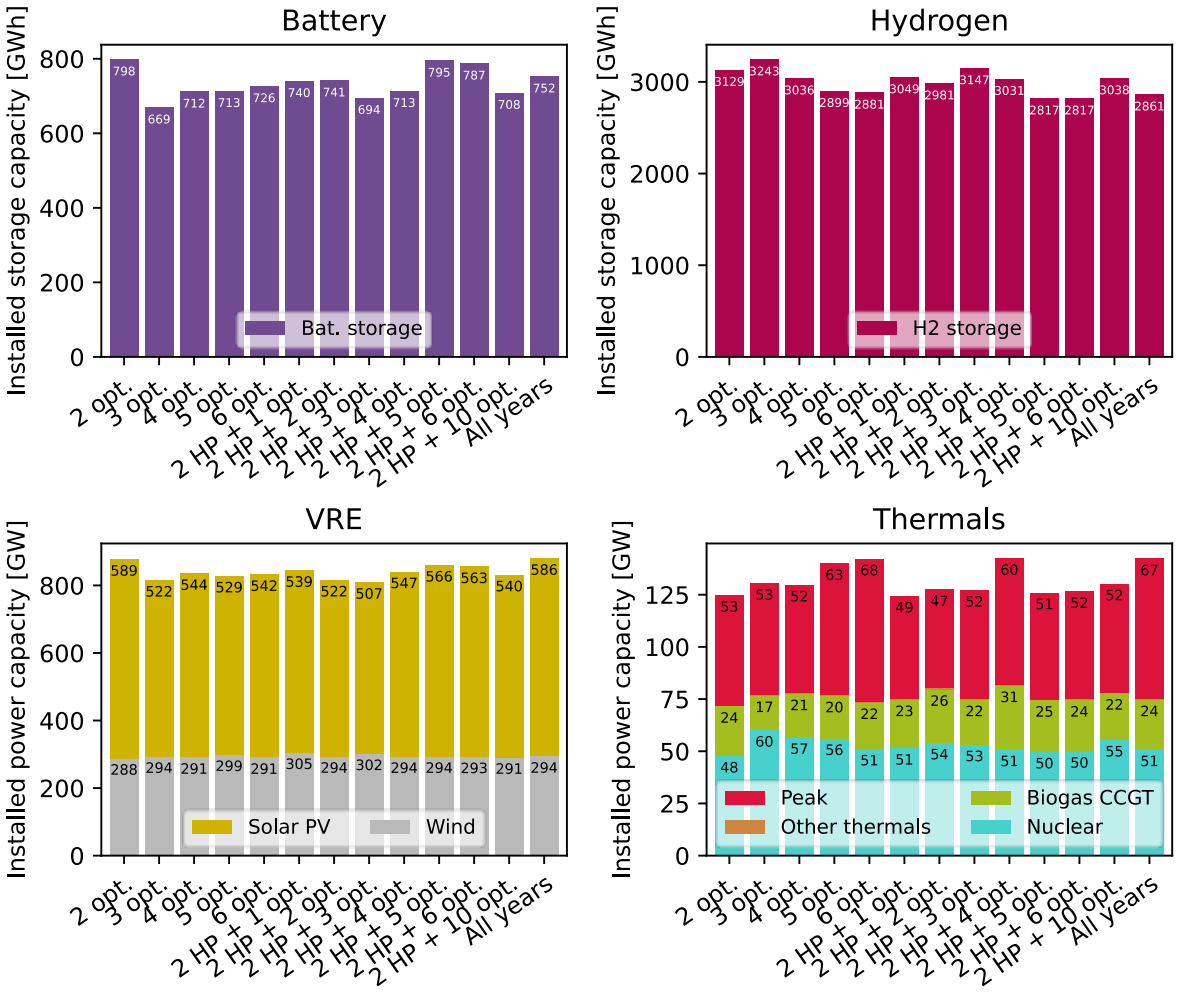

Figure 9. Installed storage and generation capacities for the sets of weather-years presented in Table 9, as well as for *All years*. The battery power capacity is not shown but is found to scale with the battery storage capacity at a ratio of ca. 6.3 GWh per GW.

While there is value associated with using a weather-year (or set) that ably represents *All years,* there is also a value in knowing the areas for which the degree of representation is poor, as well as in knowing how large the error is. For example, if it is known that, using Year A, the capacity level of a certain technology is under-estimated by 20%–25%, this might be preferable to using Year B for which the error is <20% but could be anywhere between -20% and +20%. To obtain an overview of how the extent of representation varies for sets of weather-years and for individually modelled weather-years, the variations in capacity mix, biogas use, system cost, and gross electricity trade between the Nordic countries and Continental Europe are illustrated using box-and-whisker plots in Figure 10. The box plots indicate: the 1st to 3rd quartiles (blue boxes); the median capacity level (orange line); and the distance to the furthest data-point within 1.5-times the IQR[22] (whisker). Outliers are shown as circles. All values are normalised

[22] The inter-quartile range (IQR) is the distance from the 1st to the 3rd quartiles, and the whisker extends only to the furthest data-point that extends to 1.5-times the IQR from the 1st or 3rd quartile. For an illustration of the IQR, see https://matplotlib.org/stable/api/_as_gen/matplotlib.pyplot.boxplot.html.

such that the levels of *All years* equal one. Ideally, the boxes and whiskers are small (low variance) and close to *All years* (the black horizontal line in Figure 10).

Comparing the box plots for the individually modelled years with those for the weather-year sets reveals substantial differences. These differences are evident in terms of both the variability and the median representation to *All years*, with the sets of weather-years being favoured in both aspects. The largest difference in capacity level between the sets and *All years* relates to the peak thermal capacity which, for sets with hand-picked years, is under-estimated by around 20%. The solar PV capacity is also consistently under-estimated (by around 10%) for the sets with hand-picked years. Comparing the sets with and without hand-picked years shows little difference, except for slightly larger variances in the sets without hand-picked years. The slight mis-representation of nuclear power and mid-load thermal power for the all-optimised sets seen in Figure 9 is also reflected in Figure 10. Finally, a comparison of the system cost levels shows that though there is some variability across the individual weather-years, the median is very close to the system cost of *All years*. Figure 10 also shows that sets of weather-years, despite their differences in system composition, result in almost exactly the same system cost as that of *All years* (81.5 G€ per year).

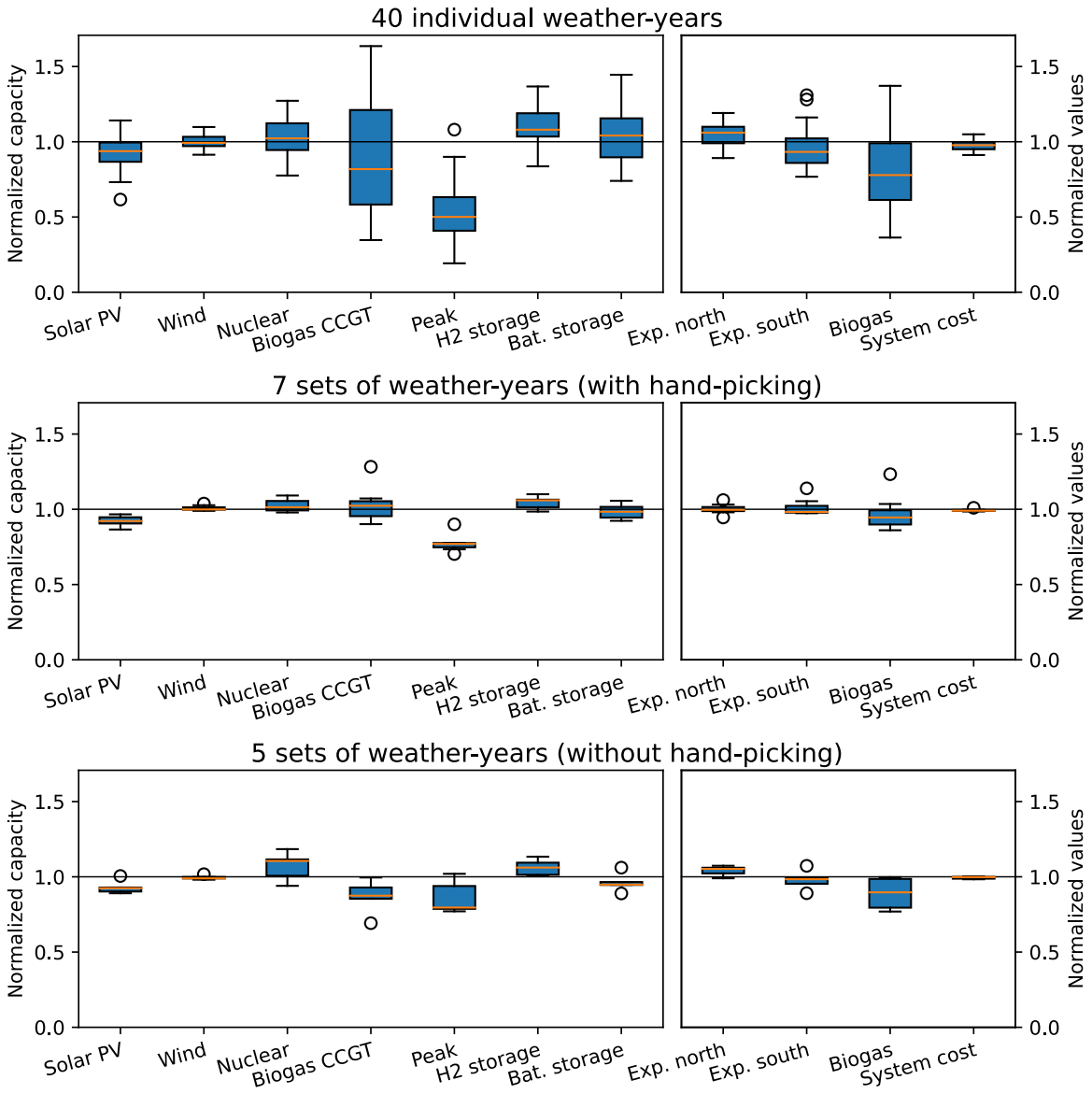

Figure 10. Box plot showing the investment levels for individual weather-years and sets of weather-years, normalised to the investment levels for *All years.* The yearly biogas use is also shown, together with the gross electricity transfer from northern Continental Europe (DE_N in Figure 4) to the Nordic countries (SE_S and NO_S in Figure 4).

4.3 Key technologies to manage inter-annual variability

KEY MESSAGE. **Paper IV** finds that when challenging weather-years are included in electricity system optimisation modelling and their probability of occurrence is accounted for, the largest impact on system composition is an increase in peak thermal capacity. This effect arises specifically for weather-years that, when modelled in isolation, result in high thermal capacity levels. Inter-annual variability is managed in the modelling through a combination of fuel storage (not explicitly modelled) and curtailed generation.

The results in **Paper IV** (Figure 7 and Table 7 therein) show that when particularly challenging weather-years are modelled in isolation, the measure applied to meet these challenging events is to increase the capacities of technologies with relatively low costs per energy unit, such as nuclear, wind and solar power. However, when the challenging weather-years form part of a set in which the probability of their occurrence is accounted for, the challenging net-load events are covered by technologies that have low costs for capacity (albeit high costs for energy), such as peak-load and mid-load biogas turbines. Notably, the cost-optimal nuclear and VRE investment levels of *All years* is very close to the median for all individually modelled weather-years, as illustrated in Figure 10. As a result, biogas turbines become a critical technology for managing inter-annual variability, along with the curtailment of potential VRE and nuclear generation during less-challenging years. The use of biogas to ensure flexibility also makes the dimensioning and management of biogas production and storage crucial for tackling inter-annual variability.

With biogas turbines as a key technology to manage rare net-load events of long duration, it is relevant to investigate both the distribution of biogas use and the fuel storage size required to supply these biogas turbines. In Figure 11, the distribution of biogas use in *All years* is illustrated as a box-and-whisker plot. The biogas consumption ranges from 25 TWh to 136 TWh, with a median consumption level of 66 TWh (indicated with an orange line in Figure 11) and mean consumption of 68 TWh (not shown). The 1st to 3rd quartiles (illustrated as a blue box in Figure 11) indicate that half of the weather-years fall within 40–80 TWh of biogas consumption, although four outliers are found above 125 TWh.

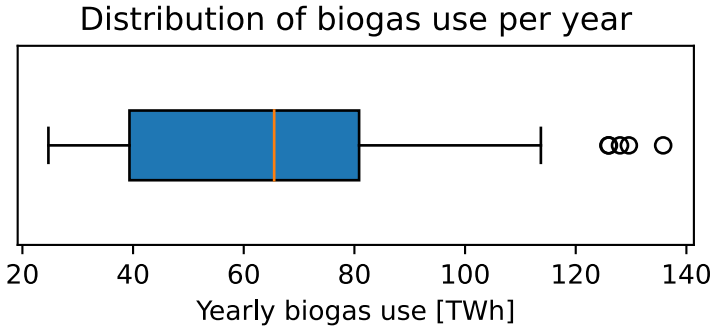

Figure 11. Distribution of biogas use in each weather-year in the *All years* model-run. The distribution is shown as a box-and-whisker plot with a median of 66 TWh (orange line).

Though biogas storage is not included in the model, its hourly storage level and the required total storage capacity can be approximated using the in-flow and out-flow values. Assuming that biogas production capacity is expensive and that storage capacity is at a relatively low cost, the production of biogas can be estimated from the average biogas consumption rate (68 TWh/year). This constant biogas production (or storage re-fill) rate can then be combined with the hourly consumption level (generated by the model) to produce a storage level curve. In

Figure 12, such a storage level curve is shown, revealing that a 235-TWh storage unit is sufficient to ensure the electricity and heat supply of Northern Europe if all the studied weather-years are connected in consecutive order. However, the storage level curve also shows that 70 TWh of storage capacity can be avoided if the re-fill rate is increased by 5 TWh/year (or 7%). This would reduce the total storage capacity requirement to 165 TWh for the electricity and heat supply in Northern Europe for the 39 weather-years investigated. For reference, the current natural gas storage capacity is 250 TWh in Germany and 139 TWh in The Netherlands [74]. In addition, 68 TWh per year is well below some estimates of potential biogas production in the modelled countries in Year 2050 (reported as 400–450 TWh in [75], [76]). It should be noted that bio-fuelled power is the only option for flexible thermal power in the model, other than hydrogen fuel cells. Natural gas is not included in the model but could, in reality, fill the same role as biogas if deemed politically acceptable. If used without carbon capture and storage, to the same extent as the modelled biogas (1.3% of the total electricity supply), natural gas combustion would result in 13.8 Mt of CO_2 emissions and a total carbon intensity of 5 g_{CO2}/kWh_{el}. The use of bioenergy for the purpose of flexibility is discussed further regarding the model limitations in Section 5.2.

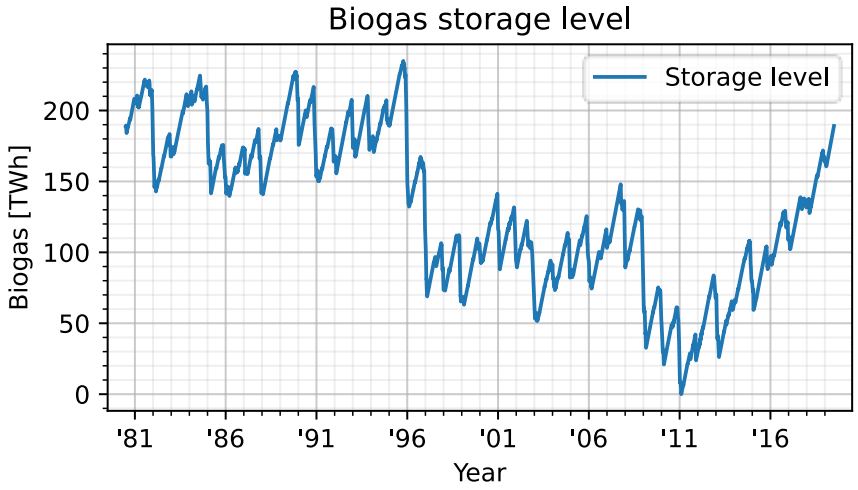

Figure 12. Biogas storage level curve assuming a constant re-fill rate of 68 TWh per year.

5. DISCUSSION

The results described in **Papers I–IV**, and presented in this thesis, provide insights into grid frequency control (short-term load balancing) and inter-annual variability in future, carbon-neutral electricity systems.

The weak contributions to grid stability obtained from wind power and solar PV relate to their non-dispatchability and their grid-connectivity through inverters rather than synchronous generators. Unless some of the available power from wind and solar generation is curtailed, their contributions to frequency reserves (FR) are limited. However, as shown in **Paper II**, this is not necessarily an expensive problem to solve. By allowing FR to be supplied from grid-scale batteries and consumers, using electrolysers for hydrogen production and power-to-heat for district heating, the demand for reserve power can be met with limited additional investments. Furthermore, the results indicate (for all modelled stages of the transition) that no additional investments or fuel costs are needed if part of the electrified car fleet (tested at 30%) participates in the FR supply. To limit the scope of that work, electrified household heating and other thermostatically controlled loads were not considered, despite representing a significant potential source of reserve power [77]. Considering these results, the supply of FR may simply become a question as to which electricity consumers will require the lowest price-to-participate, if participation from small-scale consumers is facilitated. More research is undoubtedly needed to determine the degree to which demand-side sources should be relied upon for frequency control.

However, batteries, heat pumps and electrolysers cannot provide the synchronous inertia present in the current fleet of thermal power plants. While this is an important aspect for the transition from synchronous generators to inverter-based generators, replacing the inertia is unlikely to be costly, even if it is replaced by new mechanical inertia. As argued by Brown et al. [10] and confirmed by the modelling in **Paper I** as well as a later study by Thiesen [78], mechanical inertia can be supplied by synchronous condensers at a relatively low cost. Since alternative sources of both mechanical and synthetic inertia are available, synchronous condensers represent an upper limit to the grid stability cost associated with lost inertia, while simultaneously providing reactive power and short-circuit current. Brown et al. [10] have provided a high estimate of this upper limit as 0.3 €/MWh of the total electricity consumption per year in Great Britain. **Paper I** finds that the system cost of supplying inertia using synchronous condensers is lower, at approximately 0.1 €/MWh of total electricity consumption, when evaluated in four separate and isolated regional cases across Europe. Thiesen [78] has applied an economic dispatch model to three scenarios of future German electricity systems, one of which features 100% RE (includes wind, solar, hydropower and bioenergy) for electricity generation. Thiesen [78] has shown that: (i) a short activation time (2 s instead of 30 s) of the primary reserves is important to limit the cost of inertia in all scenarios;

and (ii) for reserves with activation time of 2 s, the 100% RE scenario has the lowest additional costs related to providing inertia (0.04–0.1 €/MWh), despite a higher inertia requirement (larger N-1). While these studies support the idea that system inertia can be supplied at low cost, the efficient distribution and control of these inertia sources may still present a practical challenge and represent a knowledge gap. In particular, the direct connection between system inertia and the rate of change of frequency means that reducing the activation time of the reserve power could be crucial to limiting the cost associated with lost mechanical inertia.

As electricity systems transition to weather-dependent generation, the extent of inter-annual variability increases, while the extent of dispatchable generation (an option to manage inter-annual variability) decreases. While multiple studies have been conducted on the topic of inter-annual variability (e.g., [54]–[57], [78]–[84]), only a few[23] have applied large sets of weather-data to compare the cost-optimal investment levels of individually and simultaneously modelled weather-years. These studies have found that: (i) there are large variabilities in the capacity mixes and system costs between individually modelled weather-years; and (ii) the mean/median investments from individually modelled years differ from the investments deduced by incorporating the inter-annual variability into the cost-optimisation. The same results are found in **Paper IV**. However, there is limited information regarding how the use of dispatchable generation varies between weather-years and how the prospect of nuclear power is affected by inter-annual variability in carbon-neutral electricity systems. Ruhnau & Qvist [84] and Dowling et al. [85] have modelled 100% RE systems with inter-annual variability and dispatchable generation in the form of power-to-hydrogen-to-power with salt cavern storage. They have both found that accounting for inter-annual variability roughly doubles the required long-term storage capacity (as compared to the median of the individual years) to a size equivalent to 24–33 days of average electricity load[24]. The same results are found in the present work for the biogas storage required to enable the flexible use of gas turbines, although it is likely that the storage size would smaller if its investment cost was included in the optimisation. However, unlike the previous studies, the results herein show also how the need for dispatchable generation varies between weather-years in a system that is designed to be optimised for decades of inter-annual variability. Furthermore, by allowing for nuclear power investments in the model[25], the results indicate that inter-annual variability does not shift the cost-optimal electricity supply away from weather-dependent generation and towards nuclear power, as long as a flexible source of dispatchable generation is available.

By analysing the hourly net load of each weather-year, the method applied in **Paper IV** allows for the identification of years with particularly challenging weather-events. In so doing, **Paper IV** is able to test the hypothesis that states that explicitly including particularly challenging weather-years makes sets of weather-years (as constructed in **Paper IV**) more-representative. Figure 10 shows that weather-year sets with hand-picked years yield more-representative nuclear and mid-load capacities, and overall smaller variations between sets of different sizes, as compared to weather-year sets without hand-picked years. However, both categories of sets generally under-estimate the capacities of peak-load gas turbines. The method used to select

[23] Specifically, the following studies: [55], [56], [80], [84], [85]

[24] For reference, the 165–235 TWh of fuel storage found in **Paper IV** corresponds to 23–33 days of average electricity load.

[25] The modelling choice to include nuclear power investments is further discussed regarding the model limitations in Sub-section 5.2.2.

the dimensioning low-probability weather-years (recall the recurrence matrix from Sub-section 3.3.1) thus appears to provide a reasonable representation of long-duration events but a poor representation of the net-load peak. A better method for representing the net-load peak might be to include the weather-year (or day) with the hour of highest net-load. The identification of particularly challenging weather-years also enables a comparison of the investment levels when challenging weather-years are modelled in isolation versus when the probability of these years is accounted for in the model. It is found that neither challenging weather-years nor "normal" weather-years produce investment levels similar to those of *All years*.

Lastly, the set-building algorithm presented in **Paper IV** and herein provides a way for modellers to capture the effect of inter-annual variability without the need to model decades of weather-years. The evaluation shows that the effect of inter-annual variability on investment levels can to a large extent be captured using sets that contain only a few weather-years. However, for appropriate representation of inter-annual variance in operation-related indicators, such as biomass use[26] and greenhouse gas emissions, the weather-year sets may not suffice. Time-series aggregation (TSA) using representative days (RDs) may be an attractive alternative to represent inter-annual variability [56]. While there are methods to maintain the chronology using RDs, the feasibility of doing this while representing decades of weather-data is not yet demonstrated. The other aggregation method mentioned in Section 2.1, priority chronological time-period clustering (PCTPC), has the benefit of inherently preserving the chronology but does not have a mechanism to represent additional years' time-series without incurring a corresponding increase in the number of time-steps. As such, it is not clear how to best capture the need for inter-annual storage without having a drastic increase in the number of time-steps. However, by combining the sets of weather-years of this work with PCTPC or RDs, the variance and inaccuracy of investment levels from individually modelled weather-years may be greatly reduced, while the support for short-term and seasonal storages is maintained.

5.1 Optimisation versus simulation

While this work uses optimisation modelling, an alternative tool that has been used for some energy and power system analyses is simulation modelling. In particular, simulation models are commonly used in power engineering to calculate power flow, voltage levels, and the need for additional grid support to maintain nominal voltage levels. Simulation tools are also used to assess how a certain grid state (i.e., loads and generation at each node) responds to a disturbance.

The principal difference between optimisation models and simulation models relates to how the output is generated. While optimisation models always minimise (or maximise) an objective value to find the best solution to some problem, simulation tools use mathematical descriptions of a system and its behaviours to calculate a state or development (sometimes iterating to solve numerically complex non-linearities). This, in turn, lends the two models to different applications. For example, weather forecasts, power-flow analyses, computational flow dynamics, and the validation of algorithms for self-driving cars all use simulations. An important difference between simulation models and optimisation models lies in the ability of

[26] While the average biomass use may be well-approximated, the dimensioning of inter-annual fuel storage is not captured and may require a fundamentally different time-series aggregation approach.

the former to deal with non-linearity. While simulated systems may have degrees of freedom or require simplifications, they are not as strongly affected by non-linearity as are optimisation models. This is due to the need for a solver algorithm in optimisation modelling, whereby the most-effective algorithms use features of linearity to simplify the process. For this reason, AC power flow is not typically included in electricity system optimisation models. Instead, a simpler DC power flow implementation may be used, or the optimisation model can allow for free trade up to the net transfer capacity of the transmission lines. Grid frequency control is also affected, being generally only considered in terms of ensuring sufficient reserves or inertial power capacity, if at all. However, if the research question relates to the impacts on the optimal system design or operation, optimisation modelling cannot easily be avoided.

To combine the more-detailed operational analysis of simulation tools with the optimal system design insights gained from optimisation tools, some studies use both strategies. Often, the simulation tool is then used to validate the operability or feasibility of the system design derived using the optimisation model. However, this does not necessarily improve the optimisation model outcomes. A possible method to combine the more-detailed analysis of simulation tools with the optimal system design insights of optimisation tools is to employ a simulation tool during the development of the optimisation model. This can inform the modeller regarding how certain assumptions and simplifications made in the optimisation model affect the feasibility of the system; information which might be used to tune the model so as to compensate for the simplifications made. For example, a simulated fault in the grid might reveal that the short-circuit current is too low in a specific scenario, prompting the modeller to add new constraints (or tighten existing constraints). While this may improve the model and yield more-realistic results, this iterative process significantly increases the workload for the modeller, and its usefulness depends not only on the research question but also on the regional scope and resolution. If the regional resolution of the optimisation model does not match that required to obtain meaningful results from the simulation model, the capacity and its operation must be divided among the sub-regions (or grid buses). This introduces an additional source of error, meaning that a lack of feasibility in the simulation no longer necessarily means that the results from the optimisation model are non-feasible.

Studies that consider operability in electricity system models with investment optimisation can instead simply accept that the model results are not sufficient for real-world grid operation. The differences between the model results and a real-world operable system include additional (hidden to the model) costs and, potentially, additional capacity investments. However, this does not necessarily affect the usefulness of the results unless the hidden costs are both: (a) significant in relation to the system cost; and (b) significantly different for different system compositions. If the hidden costs fulfil both (a) and (b) they may shift the cost-balance between technologies such that sub-optimal technologies are preferred in the optimal solution. The magnitude of this shift would depend on the relative size of the hidden costs, although it is (technically) possible for near-optimal model solutions to be entirely different from the optimal solution. To limit this potential error, it is important that all costs that may differ between technologies (in terms of both the power and energy supplied) are represented where possible. When this is not possible, knowledge of the mis-representation and its extent is important in the analysis of the results, so that the modeller can know in which ways the results are skewed.

5.2 Model limitations

The modelling activities in **Papers I–IV**, though performed with different models, share the following key limitations (first presented in Section 1.3): perfect foresight; model size and complexity; and access to input data. These limitations (and others) affect, to varying degrees and in different ways, both the investigations of grid frequency control in **Papers I–III** and the investigation of inter-annual variability in **Paper IV**.

5.2.1 Perfect foresight

Perfect foresight affects the modelling of both frequency control and inter-annual variability and is mentioned in the *Discussion* section of each paper. In short, perfect foresight means that the supply of reserves can be perfectly planned, knowing before-hand both the exact demand and that no reserves are activated (the effects of the latter are investigated in the sensitivity analysis in **Paper II**). Perfect foresight also removes uncertainty about potential inter-annual variability from the system design stage. Instead, it is known exactly what the worst actual case is, so that no un-necessary investments are made which, in turn, leads to the system cost impact of inter-annual variability being under-estimated. However, the solution to challenging low-probability weather-years described in **Paper IV** is largely based on fuel storage units and thermal technologies that have low investment costs. The low investment costs of these technologies limit the hidden cost of uncertain inter-annual variability. It is, however, important that electricity systems, regardless of the main power supply, have a contingency plan to deal with unexpectedly challenging situations.

5.2.2 Limited scope, resolution and model complexity

The model scope, resolution and complexity (e.g., additional equations or non-linear variables) all directly affect the model size and the computational effort required to solve the model. As such, increasing the complexity of one dimension may require reducing the complexity of another dimension. This affects the investigations in all the papers (**Papers I–IV**), resulting in the model scopes and resolutions listed in Table 1. In **Papers II** and **III**, this limitation most notably leads to the modelling of three separate geographical regions rather than all of Europe, with some regional nodes being combined (as illustrated in Figure 3) and some model features being deactivated or simplified (e.g., no explicit modelling of heat storage units for district heating networks). As each model region in effect acts as a copper-plate (i.e., neglecting all internal transmission bottle-necks), the combining of regions may lead to the system impacts of limited transmission capacity being under-estimated. As a consequence, attempts have been made, when combining regions, to preserve the transmission bottle-necks that have the highest estimated impacts. The limited geographical scope also has a particular impact on regions on the edge of the scope, which, in reality, are inter-connected with regions outside of the scope. The region of southern Germany (DE_S), which is included in **Paper IV** but not in the preceding studies, is a notable example. The high electricity demand of DE_S in combination with its limited access to renewable energy leads to additional wind and solar investments in northern Germany (as might be expected). However, the limited transmission capacity and the lack of modelled neighbouring countries to import from makes large nuclear power investments necessary in DE_S, to satisfy the demand for electricity. Due to the need for a limited scope and the lack of satisfactory alternatives, this modelling artefact was left as-is.

The electricity system transition modelled in **Papers II** and **III**, which starts from a dispatch-only run using real-world generation capacity and advances in short-, mid- and long-term future time-steps, is (in addition to the geographical scope) affected by the need to decrease the number of discrete technologies. This simplification is made by combining all pre-existing capacities (both real-world and from previously modelled years, if any) of the same technology type (e.g., biomass CHP) to one aggregate capacity. The resulting capacity is then assigned an average efficiency, weighted by the capacities. As a result, the model only has two versions of each generation technology: pre-existing capacity, and new investments. This implementation preserves the difference in efficiency between the new and old capacities, although it somewhat mis-represents the running costs of the newest and oldest pre-existing capacities.

Another notable simplification of the technology representation made in the ENODE and Multinode models is not considering carbon dioxide removal (CDR) systems. According to the IEA [86], CDR (a form of carbon management) is a key component of all credible pathways to limit global warming to 1.5°C by Year 2100. CDR is an energy-intensive process and is expected to be implemented as a combination of bioenergy carbon capture and storage (BECCS) and direct air carbon capture and storage (DACCS). Since BECCS produces electricity and DACCS consumes electricity, their strategic use can assist in managing net-load variations [87]. However, their interactions with both the electricity and CO_2 balances add an additional source of complexity to the model. When studying the impacts of frequency control and inter-annual variability on the electricity system cost and design, this added complexity was not considered to be warranted.

The model implementation of bioenergy for dispatchable generation is related to the exclusion of CDR. Since the supply of bioenergy is limited, it is common practice to limit the amount of bioenergy available for electricity and heat production in electricity system models. When modelling future years, this might be achieved by using estimates of the future supply (at different price levels) and subtracting the estimates of the demands in non-electricity sectors. Since CDR both competes with biogas turbines for the bioenergy supply and provides an alternative to manage net-load variability, reserving the bioenergy needed for CDR without accounting for the flexibility inherent to CDR might not result in a more-accurate representation than doing neither one nor the other. Furthermore, there are uncertainties regarding the future of dispatchable generation in terms of whether natural gas should be used, and if so, whether its emissions should be compensated for with additional CDR or captured using CCS. For these reasons, all fossil fuels and negative emissions targets are excluded from the modelling in **Paper IV**, and bioenergy is implemented with an estimated market price (40 €/MWh for wood chips and 77 €/MWh for biogas). This limits the complexity of both the model and the analysis of the modelling results. For reference, the average biogas usage in *All years*, 68 TWh, corresponds to roughly 100 TWh of biomass. Although this is far lower than some estimates (e.g., [75], [76], [88], [89]) of the potential supply in Europe (as well as the scope herein) in Year 2050, it should not be assumed that this use of bioenergy is resource-optimal.

5.2.3 Other limitations

For the impacts of frequency control on the system cost, design and operation to be accurately reflected in the model, both the demand and supply should be well-represented. For the supply of FR, not only is the available capacity needed but also the cost associated with its use. While

this cost is mostly linked to the wear-and-tear and opportunity costs for some technologies (e.g., grid-scale batteries, electrolysers, and power-to-heat for district heating), it may hinge on a partly subjective price-to-participate when involving private households and vehicles. Due to the uncertainty of this price-to-participate, FR supplied by small-scale consumers were not considered in the main analysis in **Papers I–III**. The activation time must also be determined for each potential source of reserves; a determination that is complicated by a lack of experience with using demand-side technologies to provide reserves, and technologies whose activation times rely on acceptable levels of incurred wear-and-tear.

The demand for FR is intentionally set at the high end in the present work. Due to uncertainties regarding the future demand and supply of FR and due to the importance of grid stability, an over-estimated demand may be more valuable than an under-estimated demand. This is especially true when one considers that the reserves are only required to be available (not activated) and that the model has perfect foresight. It is, thus, assumed that all potential sources of reserve demand add to each other. In other words, there should be sufficient reserve power to deal with a dimensioning fault while, simultaneously, in all regions, there is a power deficiency due to the ramping of wind and solar power and stochastic load variations that are at their highest levels. The reserve demand that results from ramping wind and solar power, while not increasing significantly the median reserve demand, causes the peak reserve demand to reach 26 GW during 1 hour in the Nordic regional cases in **Papers II** and **III**. Still, additional reserves required to compensate for the non-dispatchability of wind and solar power were not found to impact negatively their shares of electricity generation. In a study conducted by Gonzato et al. [51], different model implementations of operating reserves were compared in terms of levels of investment in generation, the supplied reserves, and system cost. They found that the more-complex implementations, those that considered activation costs, relied less on reserves from peak thermal power compared to implementations that did not consider the activation cost. As the results in **Papers I–III** did not identify peak-thermals as more-competitive than batteries, not featuring an inherent activation cost, a more-complex implementation may not be warranted in **Papers I–III**. It should be noted that the models used by Gonzato et al. [51] did not feature any storage or demand-side sources of reserves (other than load shedding).

A notable limitation of the algorithm proposed in **Paper IV** is the use of a single net-load time-series per weather-year. The algorithm, as is, aggregates all the regional loads and non-dispatchable generation when building the net-load recurrence matrix, thereby neglecting all transmission bottle-necks. This is done to avoid an additional regional dimension in the matrix, without which the visual analysis and set-building optimisation are considerably easier tasks. The only apparent alternative is to calculate the net-load on a regional basis, either without electricity transmission between regions or with electricity transmission generated by some optimisation or simulation model. Given that the generation and storage capacity mix already is available (and used to calculate the non-dispatchable generation), generating transmission time-series for each weather-year in each iteration should not be an insurmountable task. Utilizing the MIQCP formulation of the set-building optimisation problem in the subsequent algorithm step, the additional matrix dimension should not be too great an issue. In addition, if needed, the set-building optimisation can be expedited by limiting the number of years in each set or by reducing the resolution of duration or amplitude in the matrix. Still, the evaluation of the weather-year sets in **Paper IV** and in Section 4.2 indicate that the Multinode model results

using weather-year sets consistently resemble *All years* better than almost all the individual weather-years. The afore-mentioned modifications are thus, in all likelihood, not warranted unless a considerably larger regional scope is applied.

5.3 Considerations for future research

The work presented in this thesis can be connected to, as well as improved upon. In terms of quantifying the real cost of frequency control, subject to specific regulations governing the demand and supply of inertia and reserves, as the shares of wind power and solar power increase, further work is needed. While the work herein adopts a technical perspective on the potential reserve supply and demand in future systems, a representation that is more closely derived from current (or planned) grid codes is needed to account for restrictions imposed by local grid codes and market restrictions. Depending on the degrees of willingness of system operators to accommodate decentralised demand-side sources of reserve power, further research into their potential capacities, and associated costs, could also be valuable. On the other hand, system operators may be hesitant to implement such accommodations until presented with the potential value of a more-accommodating grid code, given the existing conditions. Another key actor in the transition of energy systems is politicians, who are under pressure to expedite the transition but also face uncertainties regarding the stability and reliability of grids with lower levels of thermal power. Research into potential policies to ensure grid stability and reliability may be of great value in guiding policy makers and the public debate during the electricity transition.

In terms of future research using generation expansion planning models, the findings of **Papers II** and **IV** indicate that the complexity added to the model by representing frequency control (as done in this work) does not appear to be warranted, unless aspects specific to frequency control are explicitly studied. The impacts on system cost and design are limited and subject to serious uncertainties regarding the future supply of reserves. A considerably greater impact on investment levels is found when simultaneously modelling multiple weather-years. As illustrated by the box plot in Figure 10, the cost-optimal investment levels are highly sensitive to the choice of weather-year when only one weather-year is modelled. By using sets of weather-years that are generated using the algorithm presented in this work, the resulting system design is both more-robust (with less variance) and more-accurate (being closer to *All years*). As previously discussed, further use of the algorithm might benefit from adjustments that explicitly include the peak net-load, as well as better support for larger geographical scopes. The algorithm also stands to benefit from being combined with other time-series aggregation methods, to reduce further the number of required time-steps.

Although some energy-intensive sectors, which traditionally use fossil fuels, are undergoing electrification to reduce their climate impacts, others will remain dependent upon liquid fuels (or virgin carbon atoms) for a considerable time going forward. If the use of fossil fuels is to phased out from these sectors in the near future, the demand for biofuels will increase dramatically from current levels. Considerable amounts of biomass[27] will also be needed for BECCS to remove CO_2 from the atmosphere. Thus, it is vital that systems to produce and distribute large amounts of sustainable biofuels are designed and built in the not-so-distant

[27] The 1.5°C pathways may require the EU power sector to achieve negative CO_2 emissions of 63–208 Mt per year by Year 2050 [95], corresponding to roughly 190–620 TWh of biomass per year.

future. On the one hand, competing demands for the limited supply of sustainable biomass could challenge the future use of biogas, as found in **Paper IV**. On the other hand, dispatchable generation will play an important role in limiting the system cost of fully carbon-neutral electricity production [90]. Although the choice of which dispatchable technology to rely upon is multi-faceted, it is possible that CDR technologies can assist in variation management [87] (especially so if CDR is allowed to vary between years). Considering how the need for biogas (or dispatchable generation) is found to vary between years in the present work, the role of CDR in managing intra- and inter-annual variability may be of interest for future studies.

6. SUMMARY AND MAIN FINDINGS

The transition to electricity generation using weather-dependent and inverter-based solar PV and wind power raises new challenges related to the stability and reliability of electricity grids. The research carried out for this thesis investigates the impacts of frequency control (**Papers I–III**) and inter-annual variability (**Paper IV**) on the cost-optimal system compositions of carbon-neutral electricity systems. This is done using linear optimisation models in a European context, though the conclusions drawn can largely be generalised.

The results indicate that while frequency control may increase the total system cost and stimulate some investments, especially in the short-term future, this does not significantly affect the relative values of the different technologies for electricity generation. Batteries, or other highly flexible short-term storage systems, are found to be crucial for limiting the system cost of frequency control as electricity systems transition towards carbon-neutrality. Due to their high efficiency levels, low activation times and the potential to double-use batteries for intra-day flexibility and reserve power, additional investments in batteries may be the main response to an increased demand for frequency reserves in the short-term. However, demand-side sources of frequency reserves (e.g., battery electric vehicles or thermostatic loads) may out-compete grid-scale batteries, although this depends on the cost of integrating the demand-side technologies into the reserve market.

Grid inertia, if not provided by inverter-interfaced sources of power, can be provided by synthetic condensers at a low system cost (ca. 0.1 €/MWh). For the choice between investing in synthetic condensers or increasing the operation of thermal power plants, the cost-optimal solution in all the modelled regions was found to be synthetic condenser investments.

In **Paper IV**, the hourly load and generation profiles from 39 weather-years are used to study how the system composition is affected by inter-annual variability and particularly challenging net-load events. In line with the results of other studies, large variability is found between individually modelled weather-years, and the median capacity mix does not match the reference capacity mix of all weather-years modelled simultaneously. By identifying the particularly challenging weather-years, **Paper IV** is further able to demonstrate that the cost-optimal measures to deal with challenging weather-events change when their rates of occurrence are accounted for in the modelling. When the probability of challenging weather-events is accounted for, extreme events mainly lead to an increased thermal peak load capacity and a higher demand for fuel. In turn, the required fuel storage capacity is increased. If existing natural gas storage units can be re-purposed for biogas, it does not seem like inter-annual variability represent a significant system cost increase, as compared to the median system cost of individually modelled weather-years.

Overall, the modelling performed in this work does not indicate that non-dispatchability is necessarily an obstacle to the cost-efficient operation of electricity systems that are dominated by wind power and solar PV. However, for this to be true, multiple sources of flexibility must be employed and operated in an efficient manner, and the current grid operation regime may need to be overhauled. Further research into forecasting and power control systems may be needed before these criteria can be addressed. Future research may also benefit from improving upon the methodology employed in this work. For example, a larger regional scope combined with additional constraints based on national policies may provide a more-accurate picture of the challenges linked to weather-dependent generation in specific regions.

REFERENCES

[1] Copernicus Climate Change Service, "Global temperature exceeds 2°C above pre-industrial average on 17 November | Copernicus." https://climate.copernicus.eu/global-temperature-exceeds-2degc-above-pre-industrial-average-17-november (accessed Dec. 21, 2023).

[2] UNFCCC, "Outcome of the first global stocktake." https://unfccc.int/documents/636608 (accessed Dec. 21, 2023).

[3] Georgina Rannard, "COP28: Landmark summit takes direct aim at fossil fuels," *BBC*, Dec. 18, 2023.

[4] REN21, *Renewables 2023 Global Status Report collection, Renewables in Energy Supply*. 2023.

[5] S. Khalili and C. Breyer, "Review on 100% Renewable Energy System Analyses—A Bibliometric Perspective," *IEEE Access*, vol. 10, pp. 125792–125834, 2022, doi: 10.1109/ACCESS.2022.3221155.

[6] C. Breyer *et al.*, "On the History and Future of 100% Renewable Energy Systems Research," *IEEE Access*, vol. 10, pp. 78176–78218, 2022, doi: 10.1109/ACCESS.2022.3193402.

[7] B. P. Heard, B. W. Brook, T. M. L. Wigley, and C. J. A. Bradshaw, "Burden of proof: A comprehensive review of the feasibility of 100% renewable-electricity systems," *Renew. Sustain. Energy Rev.*, vol. 76, pp. 1122–1133, Sep. 2017, doi: 10.1016/j.rser.2017.03.114.

[8] ENTSO-E, "Synchronous Condenser." https://www.entsoe.eu/Technopedia/techsheets/synchronous-condenser (accessed May 17, 2022).

[9] F. O. Igbinovia, G. Fandi, Z. Müller, J. Švec, and J. Tlusty, "Cost implication and reactive power generating potential of the synchronous condenser," in *Proceedings of the 2nd International Conference on Intelligent Green Building and Smart Grid, IGBSG 2016*, Aug. 2016, doi: 10.1109/IGBSG.2016.7539450.

[10] T. W. Brown, T. Bischof-Niemz, K. Blok, C. Breyer, H. Lund, and B. V. Mathiesen, "Response to 'Burden of proof: A comprehensive review of the feasibility of 100% renewable-electricity systems,'" *Renew. Sustain. Energy Rev.*, vol. 92, pp. 834–847, Sep. 2018, doi: 10.1016/j.rser.2018.04.113.

[11] L. Göransson, "Balancing Electricity Supply and Demand in a Carbon-Neutral Northern Europe," *Energies 2023, Vol. 16, Page 3548*, vol. 16, no. 8, p. 3548, Apr. 2023, doi: 10.3390/EN16083548.

[12] L. Göransson and F. Johnsson, "A comparison of variation management strategies for wind power integration in different electricity system contexts," *Wind Energy*, vol. 21, no. 10, pp. 837–854, Oct. 2018, doi: 10.1002/WE.2198.

[13] V. Walter and L. Göransson, "Trade as a variation management strategy for wind and solar power integration," *Energy*, vol. 238, p. 121465, Jan. 2022, doi: 10.1016/j.energy.2021.121465.

[14] V. Johansson and L. Göransson, "Impacts of variation management on cost-optimal investments in wind power and solar photovoltaics," *Renew. Energy Focus*, vol. 32, pp. 10–22, Mar. 2020, doi: 10.1016/j.ref.2019.10.003.

[15] P. Holmér, J. Ullmark, L. Göransson, V. Walter, and F. Johnsson, "Impacts of thermal energy storage on the management of variable demand and production in electricity and district heating systems: a Swedish case study," *Int. J. Sustain. Energy*, vol. 39, no. 5, pp. 446–464, May 2020, doi: 10.1080/14786451.2020.1716757.

[16] ENTSO-E, "2016 Survey on Ancillary Services Procurement and Electricity Balancing Market Design," 2017. https://docstore.entsoe.eu/publications/market-reports/ancillary-services-survey/Pages/default.aspx (accessed Jan. 08, 2024).

[17] ENTSO-E, "Electricity Balancing," 2017. https://www.entsoe.eu/network_codes/eb/ (accessed Jan. 08,

2024).

[18] S. I. Lupa, M. Gagnon, S. Muntean, and G. Abdul-Nour, “The Impact of Water Hammer on Hydraulic Power Units,” *Energies 2022, Vol. 15, Page 1526*, vol. 15, no. 4, p. 1526, Feb. 2022, doi: 10.3390/EN15041526.

[19] H. K. Ringkjøb, P. M. Haugan, and I. M. Solbrekke, “A review of modelling tools for energy and electricity systems with large shares of variable renewables,” *Renewable and Sustainable Energy Reviews*, vol. 96. Pergamon, pp. 440–459, Nov. 01, 2018, doi: 10.1016/j.rser.2018.08.002.

[20] N. Mattsson, “Learning by modeling energy systems,” Chalmers University of Technology, 2019.

[21] S. Pfenninger, “Dealing with multiple decades of hourly wind and PV time series in energy models: A comparison of methods to reduce time resolution and the planning implications of inter-annual variability,” *Appl. Energy*, vol. 197, pp. 1–13, Jul. 2017, doi: 10.1016/J.APENERGY.2017.03.051.

[22] M. Hoffmann, L. Kotzur, D. Stolten, and M. Robinius, “A Review on Time Series Aggregation Methods for Energy System Models,” *Energies 2020, Vol. 13, Page 641*, vol. 13, no. 3, p. 641, Feb. 2020, doi: 10.3390/EN13030641.

[23] N. Helistö, J. Kiviluoma, H. Holttinen, J. D. Lara, and B. M. Hodge, “Including operational aspects in the planning of power systems with large amounts of variable generation: A review of modeling approaches,” *Wiley Interdiscip. Rev. Energy Environ.*, p. e341, Mar. 2019, doi: 10.1002/wene.341.

[24] S. Collins *et al.*, “Integrating short term variations of the power system into integrated energy system models: A methodological review,” *Renew. Sustain. Energy Rev.*, vol. 76, pp. 839–856, Sep. 2017, doi: 10.1016/j.rser.2017.03.090.

[25] J. H. Ward, “Hierarchical Grouping to Optimize an Objective Function,” *J. Am. Stat. Assoc.*, vol. 58, no. 301, pp. 236–244, Mar. 1963, doi: 10.1080/01621459.1963.10500845.

[26] S. Pineda and J. M. Morales, “Chronological Time-Period Clustering for Optimal Capacity Expansion Planning With Storage,” *IEEE Trans. Power Syst.*, vol. 33, no. 6, pp. 7162–7170, Nov. 2018, doi: 10.1109/TPWRS.2018.2842093.

[27] Á. García-Cerezo, R. García-Bertrand, and L. Baringo, “Computational Performance Enhancement Strategies for Risk-Averse Two-Stage Stochastic Generation and Transmission Network Expansion Planning,” *IEEE Trans. Power Syst.*, vol. 39, no. 1, pp. 273–286, Jan. 2024, doi: 10.1109/TPWRS.2023.3236397.

[28] A. Garcia-Cerezo, R. Garcia-Bertrand, and L. Baringo, “Priority Chronological Time-Period Clustering for Generation and Transmission Expansion Planning Problems With Long-Term Dynamics,” *IEEE Trans. Power Syst.*, vol. 37, no. 6, pp. 4325–4339, Nov. 2022, doi: 10.1109/TPWRS.2022.3151062.

[29] M. Hoffmann, L. Kotzur, and D. Stolten, “The Pareto-optimal temporal aggregation of energy system models,” *Appl. Energy*, vol. 315, p. 119029, Jun. 2022, doi: 10.1016/j.apenergy.2022.119029.

[30] R. Domínguez and S. Vitali, “Multi-chronological hierarchical clustering to solve capacity expansion problems with renewable sources,” *Energy*, vol. 227, p. 120491, Jul. 2021, doi: 10.1016/j.energy.2021.120491.

[31] M. Moradi-Sepahvand and S. H. Tindemans, “Capturing Chronology and Extreme Values of Representative Days for Planning of Transmission Lines and Long-Term Energy Storage Systems,” in *2023 IEEE Belgrade PowerTech*, Jun. 2023, pp. 1–6, doi: 10.1109/PowerTech55446.2023.10202993.

[32] A. P. Hilbers, D. J. Brayshaw, and A. Gandy, “Reducing climate risk in energy system planning: A posteriori time series aggregation for models with storage,” *Appl. Energy*, vol. 334, p. 120624, Mar. 2023, doi: 10.1016/j.apenergy.2022.120624.

[33] S. Gonzato, K. Bruninx, and E. Delarue, “Long term storage in generation expansion planning models with a reduced temporal scope,” *Appl. Energy*, vol. 298, p. 117168, Sep. 2021, doi: 10.1016/j.apenergy.2021.117168.

[34] J. Kiviluoma *et al.*, “Impact of wind power on the unit commitment, operating reserves, and market design,” *IEEE Power Energy Soc. Gen. Meet.*, 2011, doi: 10.1109/PES.2011.6039621.

[35] D. Kirschen and G. Strbac, “Fundamentals of Power System Economics,” *Fundam. Power Syst. Econ.*, Jan. 2005, doi: 10.1002/0470020598.

[36] E. Lidstrom and D. Wall, “Frequency support by synthetic inertia from variable speed wind turbines,” in *CIRED Workshop 2016*, 2016, pp. 76 (4 .)-76 (4 .), doi: 10.1049/cp.2016.0676.

[37] A. Gloe, C. Jauch, B. Craciun, and J. Winkelmann, “Continuous provision of synthetic inertia with wind turbines: implications for the wind turbine and for the grid,” *IET Renew. Power Gener.*, vol. 13, no. 5, pp. 668–675, Apr. 2019, doi: 10.1049/iet-rpg.2018.5263.

[38] ENERCON, “Final Report Demonstrating the Value of Wind Farm Inertial Response Functionalities to the Alberta Transmission System,” 2020. Accessed: May 07, 2022. [Online]. Available: https://web.archive.org/web/20220507100637/https://albertainnovates.ca/app/uploads/2020/07/ENERCON-–-Demonstrating-the-Value-of-Wind-Farm-Inertial-Response-Functionalities-to-the-Alberta-Transmission-System.pdf.

[39] P. Fairley, “Can Synthetic Inertia from Wind Power Stabilize Grids? - IEEE Spectrum,” 2016. https://spectrum.ieee.org/can-synthetic-inertia-stabilize-power-grids (accessed May 07, 2022).

[40] G. Parkinson, “‘Virtual machine’: Hornsdale battery steps in to protect grid after Callide explosion | RenewEconomy,” 2021. https://reneweconomy.com.au/virtual-machine-hornsdale-battery-steps-in-to-protect-grid-after-callide-explosion/ (accessed May 07, 2022).

[41] Svenska Kraftnät, “Snabb frekvensreserv (FFR),” 2023. https://www.svk.se/aktorsportalen/bidra-med-reserver/om-olika-reserver/ffr/ (accessed Jan. 09, 2024).

[42] P. Daly, D. Flynn, and N. Cunniffe, “Inertia considerations within unit commitment and economic dispatch for systems with high non-synchronous penetrations,” in *2015 IEEE Eindhoven PowerTech*, Jun. 2015, pp. 1–6, doi: 10.1109/PTC.2015.7232567.

[43] S. C. Johnson, J. D. Rhodes, and M. E. Webber, “Understanding the impact of non-synchronous wind and solar generation on grid stability and identifying mitigation pathways,” *Appl. Energy*, vol. 262, p. 114492, Mar. 2020, doi: 10.1016/J.APENERGY.2020.114492.

[44] J. Tan, Y. Zhang, S. You, Y. Liu, and Y. Liu, “Frequency Response Study of U.S. Western Interconnection under Extra-High Photovoltaic Generation Penetrations,” in *2018 IEEE Power & Energy Society General Meeting (PESGM)*, Aug. 2018, pp. 1–5, doi: 10.1109/PESGM.2018.8586163.

[45] Directorate-General for Energy, “Estonia, Latvia & Lithuania agree to synchronise their electricity grids with the European grid by early 2025.” https://energy.ec.europa.eu/news/estonia-latvia-lithuania-agree-synchronise-their-electricity-grids-european-grid-early-2025-2023-08-03_en (accessed Jan. 09, 2024).

[46] ENTSO-E, “ENTSO-E Balancing Report,” 2020. Accessed: Jan. 09, 2024. [Online]. Available: https://eepublicdownloads.entsoe.eu/clean-documents/nc-tasks/2020_Balancing_report_5d242f125b.pdf.

[47] A. Van Stiphout, K. De Vos, and G. Deconinck, “The Impact of Operating Reserves on Investment Planning of Renewable Power Systems,” *IEEE Trans. Power Syst.*, vol. 32, no. 1, pp. 378–388, Jan. 2017, doi: 10.1109/TPWRS.2016.2565058.

[48] P. González-Inostroza, C. Rahmann, R. Álvarez, J. Haas, W. Nowak, and C. Rehtanz, “The Role of Fast Frequency Response of Energy Storage Systems and Renewables for Ensuring Frequency Stability in Future Low-Inertia Power Systems,” *Sustain. 2021, Vol. 13, Page 5656*, vol. 13, no. 10, p. 5656, May

2021, doi: 10.3390/SU13105656.

[49] S. T. P. Løvengreen, “Security-constrained expansion planning of low carbon power systems,” Melbourne School of Engineering, 2021.

[50] E. Raycheva, J. Garrison, C. Schaffner, and G. Hug, “HIGH RESOLUTION GENERATION EXPANSION PLANNING CONSIDERING FLEXIBILITY NEEDS: THE CASE OF SWITZERLAND IN 2030,” in *IET Conference Proceedings*, Jan. 2020, vol. 2020, no. 5, pp. 416–421, doi: 10.1049/icp.2021.1256.

[51] S. Gonzato, K. Bruninx, and E. Delarue, “An improved treatment of operating reserves in generation expansion planning models,” in *2020 International Conference on Probabilistic Methods Applied to Power Systems (PMAPS)*, Aug. 2020, pp. 1–10, doi: 10.1109/PMAPS47429.2020.9183389.

[52] B. Shirizadeh and P. Quirion, “The importance of renewable gas in achieving carbon-neutrality: Insights from an energy system optimization model,” *Energy*, vol. 255, p. 124503, Sep. 2022, doi: 10.1016/j.energy.2022.124503.

[53] D. Groppi, F. Feijoo, A. Pfeifer, D. A. Garcia, and N. Duic, “Analyzing the impact of demand response and reserves in islands energy planning,” *Energy*, vol. 278, p. 127716, Sep. 2023, doi: 10.1016/j.energy.2023.127716.

[54] P. J. Coker, H. C. Bloomfield, D. R. Drew, and D. J. Brayshaw, “Interannual weather variability and the challenges for Great Britain’s electricity market design,” *Renew. Energy*, vol. 150, pp. 509–522, May 2020, doi: 10.1016/j.renene.2019.12.082.

[55] M. Zeyringer, J. Price, B. Fais, P.-H. Li, and E. Sharp, “Designing low-carbon power systems for Great Britain in 2050 that are robust to the spatiotemporal and inter-annual variability of weather,” *Nat. Energy*, vol. 3, no. 5, pp. 395–403, Apr. 2018, doi: 10.1038/s41560-018-0128-x.

[56] A. P. Hilbers, D. J. Brayshaw, and A. Gandy, “Importance subsampling: improving power system planning under climate-based uncertainty,” *Appl. Energy*, vol. 251, p. 113114, Oct. 2019, doi: 10.1016/j.apenergy.2019.04.110.

[57] T. Brijs, A. van Stiphout, S. Siddiqui, and R. Belmans, “Evaluating the role of electricity storage by considering short-term operation in long-term planning,” *Sustain. Energy, Grids Networks*, vol. 10, pp. 104–117, Jun. 2017, doi: 10.1016/j.segan.2017.04.002.

[58] L. Göransson, J. Goop, M. Odenberger, and F. Johnsson, “Impact of thermal plant cycling on the cost-optimal composition of a regional electricity generation system,” *Appl. Energy*, vol. 197, pp. 230–240, Jul. 2017, doi: 10.1016/J.APENERGY.2017.04.018.

[59] C. Weber, *Uncertainty in the Electric Power Industry*, vol. 77. New York, NY: Springer New York, 2005.

[60] ENTSO-E, “Completing the map – Power system needs in 2030 and 2040,” 2021.

[61] J. Ullmark, “Modelling-profiles,” *GitHub*. https://github.com/jonull93/modelling-profiles.

[62] M. Taljegard, L. Göransson, M. Odenberger, and F. Johnsson, “To Represent Electric Vehicles in Electricity Systems Modelling—Aggregated Vehicle Representation vs. Individual Driving Profiles,” *Energies*, vol. 14, no. 3, p. 539, Jan. 2021, doi: 10.3390/en14030539.

[63] World Steel Association, “World Steel in Figures,” Brussels, 2019. Accessed: Nov. 03, 2023. [Online]. Available: https://worldsteel.org/wp-content/uploads/2019-World-Steel-in-Figures.pdf.

[64] Transport & Environment, “How not to lose it all: Two-thirds of Europe’s battery gigafactories at risk without further action,” Brussels, 2023. Accessed: Nov. 03, 2023. [Online]. Available: https://www.transportenvironment.org/wp-content/uploads/2023/03/2023_03_Battery_risk_How_not_to_lose_it_all_report.pdf.

[65] H. Hersbach *et al.*, “Complete ERA5 from 1940: Fifth generation of ECMWF atmospheric reanalyses of the global climate,” *Copernicus Climate Change Service (C3S) Data Store (CDS)*, 2017. .

[66] N. Mattsson, “GlobalEnergyGIS,” *GitHub*. https://github.com/niclasmattsson/GlobalEnergyGIS.

[67] N. Mattsson, V. Verendel, F. Hedenus, and L. Reichenberg, “An autopilot for energy models – Automatic generation of renewable supply curves, hourly capacity factors and hourly synthetic electricity demand for arbitrary world regions,” *Energy Strateg. Rev.*, vol. 33, p. 100606, Jan. 2021, doi: 10.1016/J.ESR.2020.100606.

[68] ENTSO-E, “Supporting Document for the Network Code on Load-Frequency Control and Reserves European Network of Transmission System Operators for Electricity 2 European Network of Transmission System Operators for Electricity,” 2013.

[69] ENTSO-E, “Rate of Change of Frequency (ROCOF) withstand capability: ENTSO-E guidance document for national implementation for network codes on grid connection,” pp. 1–6, 2017, Accessed: Nov. 29, 2021. [Online]. Available: https://www.entsoe.eu/Documents/SOC documents/RGCE_SPD_frequency_stability_criteria_v10.pdf.

[70] P. Imgart and P. Chen, “Evaluation of the System-Aggregated Potentials of Inertial Support Capabilities from Wind Turbines,” in *2019 IEEE PES Innovative Smart Grid Technologies Europe (ISGT-Europe)*, Sep. 2019, pp. 1–5, doi: 10.1109/ISGTEurope.2019.8905488.

[71] Danish Energy Agency and Energinet, “Technology Data - Generation of Electricity and District heating,” 2017. https://ens.dk/sites/ens.dk/files/Statistik/technology_data_catalogue_for_el_and_dh_-_0009.pdf (accessed Oct. 20, 2017).

[72] A. Schröder, F. Kunz, J. Meiss, R. Mendelevitch, and C. Von Hirschhausen, “Current and Prospective Costs of Electricity Generation until 2050,” 2013. Accessed: Nov. 26, 2020. [Online]. Available: https://ideas.repec.org/p/diw/diwddc/dd68.html.

[73] Y. Zhang, V. Cheng, D. S. Mallapragada, J. Song, and G. He, “A Model-Adaptive Clustering-Based Time Aggregation Method for Low-Carbon Energy System Optimization,” *IEEE Trans. Sustain. Energy*, vol. 14, no. 1, pp. 55–64, Jan. 2023, doi: 10.1109/TSTE.2022.3199571.

[74] GIE, “Gas Infrastructure Europe - AGSI.” https://agsi.gie.eu/ (accessed Oct. 04, 2023).

[75] J. Birman, J. Burdloff, H. De Peufeilhoux, G. Erbs, M. Feniou, and P.-L. Lucille, “Biomethane: potential and cost in 2050,” 2021. Accessed: Jan. 22, 2024. [Online]. Available: https://www.engie.com/en/news/study-biomethane-potential-cost-2050.

[76] European Biogas Association, “Biomethane production potentials in the EU,” 2022. https://www.europeanbiogas.eu/biomethane-production-potentials-in-the-eu/ (accessed Jan. 19, 2024).

[77] L. Herre, B. Nourozi, M. R. Hesamzadeh, Q. Wang, and L. Söder, “A bottom-up quantification of flexibility potential from the thermal energy storage in electric space heating electric power rating time a TCL takes in powered mode from one end of the deadband to the other time a TCL takes in unpowered mode from one end ,” 2021. Accessed: Apr. 29, 2021. [Online]. Available: https://orbit.dtu.dk/en/persons/lars-finn-herre.

[78] H. Thiesen, “Power System Inertia Dispatch Modelling in Future German Power Systems: A System Cost Evaluation,” *Appl. Sci. 2022, Vol. 12, Page 8364*, vol. 12, no. 16, p. 8364, Aug. 2022, doi: 10.3390/APP12168364.

[79] I. Staffell and S. Pfenninger, “The increasing impact of weather on electricity supply and demand,” *Energy*, vol. 145, pp. 65–78, Feb. 2018, doi: 10.1016/J.ENERGY.2017.12.051.

[80] A. Grochowicz, K. van Greevenbroek, F. E. Benth, and M. Zeyringer, “Intersecting near-optimal spaces: European power systems with more resilience to weather variability,” *Energy Econ.*, vol. 118, p. 106496, Feb. 2023, doi: 10.1016/J.ENECO.2022.106496.

[81] S. Collins, P. Deane, B. Ó Gallachóir, S. Pfenninger, and I. Staffell, “Impacts of Inter-annual Wind and Solar Variations on the European Power System,” *Joule*, vol. 2, no. 10, pp. 2076–2090, Oct. 2018, doi: 10.1016/j.joule.2018.06.020.

[82] I. De Palma, N. Riccio, E. E. De Tuglie, and P. Di Cicco, “Long Term Scenarios: optimal selection of a representative set of climatic years for the simulation of the National Electricity System,” *MELECON 2022 - IEEE Mediterr. Electrotech. Conf. Proc.*, pp. 659–664, 2022, doi: 10.1109/MELECON53508.2022.9843088.

[83] C. Mikovits, E. Wetterlund, S. Wehrle, J. Baumgartner, and J. Schmidt, “Stronger together: Multi-annual variability of hydrogen production supported by wind power in Sweden,” *Appl. Energy*, vol. 282, p. 116082, Jan. 2021, doi: 10.1016/J.APENERGY.2020.116082.

[84] O. Ruhnau and S. Qvist, “Storage requirements in a 100% renewable electricity system: extreme events and inter-annual variability,” *Environ. Res. Lett.*, vol. 17, no. 4, p. 044018, Mar. 2022, doi: 10.1088/1748-9326/AC4DC8.

[85] J. A. Dowling *et al.*, “Role of Long-Duration Energy Storage in Variable Renewable Electricity Systems,” *Joule*, vol. 4, no. 9, pp. 1907–1928, Sep. 2020, doi: 10.1016/J.JOULE.2020.07.007/ATTACHMENT/CE7FB308-32A7-4A52-82DE-2E9757A3431B/MMC1.PDF.

[86] IEA, “Credible Pathways to 1.5 °C,” 2023. [Online]. Available: https://www.iea.org/reports/credible-pathways-to-150c.

[87] M. Lehtveer and A. Emanuelsson, “BECCS and DACCS as Negative Emission Providers in an Intermittent Electricity System: Why Levelized Cost of Carbon May Be a Misleading Measure for Policy Decisions,” *Front. Clim.*, vol. 3, p. 647276, Mar. 2021, doi: 10.3389/fclim.2021.647276.

[88] T. Tröndle, J. Lilliestam, S. Marelli, and S. Pfenninger, “Trade-Offs between Geographic Scale, Cost, and Infrastructure Requirements for Fully Renewable Electricity in Europe,” *Joule*, vol. 4, no. 9, pp. 1929–1948, Sep. 2020, doi: 10.1016/j.joule.2020.07.018.

[89] P. Ruiz *et al.*, “The JRC-EU-TIMES model. Bioenergy potentials for EU and neighbouring countries,” p. 172, 2015, doi: 10.2790/01017.

[90] N. A. Sepulveda, J. D. Jenkins, F. J. de Sisternes, and R. K. Lester, “The Role of Firm Low-Carbon Electricity Resources in Deep Decarbonization of Power Generation,” *Joule*, vol. 2, no. 11, pp. 2403–2420, Nov. 2018, doi: 10.1016/J.JOULE.2018.08.006.

[91] C. Marcy, T. Goforth, D. Nock, and M. Brown, “Comparison of temporal resolution selection approaches in energy systems models,” *Energy*, vol. 251, p. 123969, Jul. 2022, doi: 10.1016/J.ENERGY.2022.123969.

[92] V. M. Kiss, Z. Hetesi, and T. Kiss, “The effect of time resolution on energy system simulation in case of intermittent energies,” *Renew. Sustain. Energy Rev.*, vol. 191, p. 114099, Mar. 2024, doi: 10.1016/J.RSER.2023.114099.

[93] J. J. Miettinen and H. Holttinen, “Characteristics of day-ahead wind power forecast errors in Nordic countries and benefits of aggregation,” *Wind Energy*, vol. 20, no. 6, pp. 959–972, Jun. 2017, doi: 10.1002/we.2073.

[94] K. F. Forbes and E. M. Zampelli, “Accuracy of wind energy forecasts in Great Britain and prospects for improvement,” *Util. Policy*, vol. 67, p. 101111, Dec. 2020, doi: 10.1016/j.jup.2020.101111.

[95] Climate Analytics, “1.5°C National Pathways Explorer,” 2022. https://1p5ndc-pathways.climateanalytics.org/countries/european-union/sectors/power/ (accessed Jan. 20, 2024).